Inactivation of oral biofilms using visible light and water-filtered infrared A radiation and indocyanine green

Burchard, Thomas ; Karygianni, Lamprini ; Hellwig, Elmar ; Follo, Marie ; Wrbas, Thomas ; Wittmer, Annette ; Vach, Kirstin ; Al-Ahmad, Ali

Abstract: Aim: To investigate the antimicrobial photodynamic therapy (aPDT) of visible light and water-filtered infrared A radiation in combination with indocyanine green (ICG) on planktonic oral microorganisms as well as on oral biofilm. Methods: The irradiation was conducted for 5 min in combination with ICG. Treatment with chlorhexidine served as a positive control. The number of colony forming units and bacterial vitality were quantified. Results: All tested bacterial strains and salivary bacteria were killed at a level of $3\log_{10}$. The colony forming units of the initial mature oral biofilms were strongly reduced. The high bactericidal effect of aPDT was confirmed by live/dead staining. Conclusion: The aPDT using visible light and water-filtered infrared A radiation and ICG has the potential to treat periodontitis and peri-implantitis.

DOI: https://doi.org/10.4155/fmc-2018-0522

Inactivation of oral biofilms using visible light and water-filtered infrared A radiation and indocyanine green

Burchard T[1], Karygianni L[2], Hellwig E[3], Follo M[4], Wrbas T[3], Wittmer A[5], Vach K[6], Al-Ahmad A[3*]

[1]Department of Prosthetic Dentistry, Center for Dental Medicine, Medical Center - University of Freiburg, Faculty of Medicine, University of Freiburg, Freiburg, Germany.

[2]Clinic of Conservative and Preventive Dentistry, Center of Dental Medicine, University of Zurich, Switzerland

[3]Department of Operative Dentistry and Periodontology, Center for Dental Medicine, Medical Center - University of Freiburg, Faculty of Medicine, University of Freiburg, Freiburg, Germany

[4]Department of Hematology, Oncology and Stem Cell Transplantation, Medical Center - University of Freiburg, Faculty of Medicine, University of Freiburg, Freiburg, Germany.

[5]Department of Hygiene and Microbiology, Medical Center - University of Freiburg, Faculty of Medicine, University of Freiburg, Freiburg, Germany.

[6]Department of Medical Biometry and Statistics, Faculty of Medicine, University of Freiburg, Germany.

*Corresponding author

Prof. Ali Al-Ahmad

Department of Operative Dentistry and Periodontology, Medical Center – University of Freiburg, Faculty of Medicine, University of Freiburg, Hugstetter Strasse 55, 79106 Freiburg, Germany, Phone Number: 0049 761 27048940, Fax Number: 0049 761 27047620, Email: ali.al-ahmad@uniklinik-freiburg.de

Abstract

Aim: To investigate the antimicrobial photodynamic therapy (aPDT) of visible light and water-filtered infrared A radiation (VIS+wIRA) in combination with indocyanine green (ICG) on planktonic oral microorganisms as well as on oral biofilm.

Material & Methods: The irradiation was conducted for five minutes in combination with ICG. Treatment with chlorhexidine (CHX) served as a positive control. The number of colony forming units and bacterial vitality were quantified.

Results: All tested bacterial strains and salivary bacteria were killed at a level of 3 $\log_{10}$. The CFU of the initial mature oral biofilms were strongly reduced. The high bactericidal effect of aPDT was confirmed by live/dead staining.

Conclusion: The aPDT using VIS+wIRA and ICG has the potential to treat periodontitis and peri-implantitis.

Key words: antimicrobial photodynamic therapy (aPDT), indocyanine green (ICG), oral biofilm, visible light and water-filtered infrared A (VIS+wIRA)

Introduction

Photoactivated disinfection with toluidine blue (TB) and methylene blue (MB) is currently used in dentistry to reduce the number of microorganisms in root canals, cavities and the periodontium [1–5]. Conventional mechanical treatments are unable to completly remove biofilms due to poor accessibility [6–8]. This technique was investigated because, in contrast to many chemicals used for disinfection e.g. chlorhexidine (CHX), this method is able to completely eradicate non-accessible bacteria in root canals or in cavities within the tooth. The reason for this is due to the morphology of dentin and root cement. This kind of morphology offers niches for microorganisms into which biocompatible chemicals cannot penetrate [9–11]. This often requires additional antibiotic therapy, which however, should be used only rarely and with care, especially with regard to the rise in antibiotic resistance.

Due to unfavorable outcomes correlating with the use of established oral biofilm treatments, the introduction of antimicrobial photodynamic therapy (aPDT) is considered as a noninvasive, biofilm-targeted, and affordable photochemical technique against polymicrobial oral infections, especially as an alternative to antibiotic therapy [12,13]. The aPDT can not only be used against current dental infections but also as a photodynamic disinfection during follow-up care and as prevention measure, e.g. in the field of oral surgery and implantology, to sterilize the bone cavity [14,15].

Upon illumination, the antimicrobial effect of aPDT occurs as an oxidative burst and damages biomolecules as well as other cellular structures and in a non-selective way. The aPDT necessitates the presence of three components: a non-toxic photosensitizer, molecular oxygen and visible light of a specific wavelength [2].

The aPDT can be applied either with broadband halogen lamps or light emitting diodes (LED) as light sources [16–19]. Nevertheless, the limited emission wavelength spectrum associated with cheap LED devices and broadband halogen lamps results in tissue overheating [1].

A promising alternative is the previously described combination of a wide band light source with visible light (VIS) wavelengths and water-filtered infrared A (wIRA) wavelengths [20]. The benefits of combining VIS with wIRA include increasing *in situ* temperature without thermal stress on the external tissue layers. It also increases

tissue oxygen partial pressure and improves tissue perfusion, promoting tissue regeneration and pain relief [4, 5]. The absorption spectrum of photosensitizers could be modified (shifted) after application in situ i. e. in the oral cavity. This shift should be compensated by a broadband light source like the combination of VIS and wIRA. Furthermore, wIRA is a special form of infrared radiation with high subcutaneous tissue penetration at low thermal surface load, allowing a significantly higher energy input into the tissue and showing both thermal and temperature-dependent, as well as non-thermal and temperature-independent effects [7–9].

In recent studies, high antimicrobial effects of aPDT using VIS and wIRA (VIS+wIRA) in combination with photosensitizers like MB, TB and chlorine e6 (Ce6) against planktonic and adherent microorganisms have been established [20,25]. These previous studies have shown that aPDT using VIS+wIRA shows great potential as an adjunctive therapy for peri-implantitis and periodontitis, as both the initial and mature oral biofilm have to a large extent been eradicated. Photosensitizers which are clinically approved are required to conduct clinical trials. While Ce6 is promising, it has not to date been approved for *in situ* use in the oral cavity.

Unlike other photosensitizers indocyanine green (ICG), a photosensitizer belonging to the polymethine group, has been approved by the Food and Drug Administration (FDA) [26]. ICG is a water-soluble anionic tricarbocyanine dye, which is used not only for bioimaging but also because of its near infrared absorption and its fluorescence emission properties, also as a cytotoxic photosensitizer for aPDT, when combined with light at wavelengths between 800 and 830 nm [27]. As a potential advantage over other photosensitizers, it should be noted that ICG is metabolized in the liver and has low toxicity as it is not absorbed by the intestinal mucous membrane [27]. After light absorption, the ICG molecule can follow three main pathways to deactivate its excited singlet state. The absorbed energy can be released as fluorescence emission between 750 nm and 950 nm, depending on solvent and dye concentrations. In addition, a part of the energy can be transferred to an ICG triplet state, which generates reactive oxygen species (ROS), or the energy can be transformed into heat within the ICG molecule through internal conversion [28]. In contrast to MB, TB and Ce6, most of the absorbed light is transformed into heat so that the effect of ICG is described as photothermal and photooxidative [29–31].

Thereby the depth penetration is increased compared to the other established photosensitizers.

However, most publications relating aPDT with ICG used diode lasers and are restricted to examinations of planktonic bacteria [32,33] except for a few publications examining biofilm formation [34–38].

Promising results by Omar *et al.* [39] using aPDT with ICG as a photosensitizer and a near-infrared laser (808 nm) as a light source showed a high reduction (up to 99%) of Gram-positive (*Streptococcus pyogenes, Staphylococcus aureus*) and Gram-negative (*Pseudomonas aeruginosa*) bacteria. Additionally, significant reductions in the biofilm (up to 67% for *Streptococcus mutans* and about 43% for *Enterococcus faecalis*, respectively) using aPDT with ICG and a diode laser as the light source were reported [34,35]. Until now, the suitability of this photosensitizer in combination with VIS+wIRA and its beneficial effects compared to other light sources used to kill oral or initially adherent germs has not been investigated.

In the present study the antimicrobial effect of photosensitization on pure microorganisms and total salivary flora, as well as on initial and mature oral biofilms, were investigated *in vitro* using ICG as a photosensitizer in combination with VIS+wIRA. For this purpose, pure planktonic cultures of five common oral bacteria (*S. mutans, E. faecalis*, *Eikenella corrodens, Fusobacterium nucleatum* and *Veillonella parvula*) were grown *in vitro*. In addition, initial and mature intact oral biofilms were grown on bovine enamel slabs (BES) within the oral cavity for either 2 hours (h) or 3 days (d), respectively. The planktonic bacterial cultures, total salivary bacteria, as well as oral biofilms were then treated with aPDT using VIS+wIRA in combination with ICG. The surviving bacteria from the treated initial and mature oral biofilms were determined as colony forming units (CFU), and the isolated species were identified. Additionally, for visualization and quantification live/dead staining was performed. The findings are a prerequisite for further clinical studies and essential to get knowledge about the possibility of using ICG as a photosensitizer with VIS+wIRA as an alternative to typical antimicrobial treatment methods in the field of dentistry.

Materials and Methods

Light Source and Photosensitizer

In this study, a broad-band VIS+wIRA radiator (Hydrosun 750FS, Hydrosun Medizintechnik, Müllheim, Germany) with a 7 mm water cuvette was used as previously described [20,25,40]. Instead of the usual filter, a different orange filter, BTE31, with more than twice the effective integral irradiance compared to the absorption spectrum of protoporphyrin IX, was used. Protoporphyrin IX is also included in bacterial cells and could improve the outcome of photodynamic inactivation. This has now been added to the introduction section. The continuous water-filtered spectrum with local minima at 970 nm, 1200 nm, and 1430 nm, ranged between 570 and 1400 nm [41]. The following absorption bands of IRA were removed by the water filter: 944 nm, 1180 nm and 1380 nm. This emission spectrum which has been depicted extensively in the literature [42,43] covers the broad absorbance spectrum of ICG (600-840 nm) which is depicted in Figure 1. The aPDT was applied for 5 minutes, including approximately 48 mW/cm^2 VIS and 152 mW/cm^2 wIRA, a total of 200 mW/cm^2 VIS+wIRA.

The photosensitizer used was ICG (perio green®, elexxion, Singen, Germany). Due to the contraindication of iodine allergy listed by the manufacturer, the presence of about 5% iodide is assumed, the sole purpose of which is to improve solubility [11]. ICG solutions were prepared in water for injection at different concentrations of 50 µg/ml up to 500 µg/ml. The ICG solution was stored in the dark for no longer than 4 h before use to prevent any light-induced photochemical attenuation. The optical absorption spectrum of ICG revealed maximum absorption peaks in the region from 800 nm to 830 nm [27]. The emission spectrum of this light source covers the entire absorbance spectrum of ICG (600-840 nm) which can also vary depending on the application site in the oral cavity. Furthermore, the broad emission spectrum enables efficient activation of the photosensitizer. Irradiation with VIS+wIRA activates ICG without causing an overheating of the human soft tissue. This has now been added to the depiction of the used dye. The absorption spectrum of the used ICG in water is depicted in Figure 1.

Bacterial Strains

Clinical isolates of *Enterococcus faecalis* T9 and *Streptococcus mutans* DSM 20523 were cultivated on Columbia blood agar (CBA) plates as well as *Eikenella corrodens* FB69/36-26 on yeast-cysteine blood agar (HCB) plates at 37 °C in an aerobic

atmosphere with 5% CO_2. The bacteria were derived from long-term storage at -80 °C in brain heart infusion medium containing 15% (v/v) glycerol as described earlier [44]. Further isolates of *Fusobacterium nucleatum* ATCC 25586 and *Veillonella parvula* DSM 2008 were cultivated on HCB plates under anaerobic conditions (anaerobic jars, GENbox anaer, Biomerieux Marcy l'Etoile-France). Long-term storage of these anaerobic bacteria was performed at -80°C in basal glucose phosphate (BGP) growth medium containing 15% (v/v) glycerol as described elsewhere [44].

Overnight cultures of aerobic bacterial strains were prepared in tryptic soy broth (TSB, Merck) and in GC-HP (Gas Chromatography-Hewlett Packard) bouillon for anaerobic bacterial strains. All bacterial strains were kindly provided by the Institute of Medical Microbiology and Hygiene of the Albert Ludwigs University, Freiburg, Germany. In addition, unstimulated human saliva from three healthy volunteers which had not used anti-bacterial mouth rinses or any antibiotics in the three months prior to the start of the study was investigated. The saliva and 8 ml cell suspensions of each organism were centrifuged at 4000 g for 10 minutes. Finally, after discarding the supernatant, 8 ml 0.9% saline solution (NaCl) was added.

Selection of study participants and test specimens

The study protocol was reviewed and approved by the local ethics committee (No.502 / 13). An explanation and declaration of consent were signed by all participants in advance and are available in writing.

By a preliminary clinical examination of the oral cavity, three healthy volunteers were selected to participate in the study. The exclusion criteria were defined as follows: 1) systemic disease, 2) salivary glands disorders, 3) caries or periodontal disease, 4) pregnancy or lactation, 5) smoking, 6) use local antimicrobial agents such as chlorhexidine (CHX) of antibiotics within the last three months. All participants had optimal oral hygiene prior to the study.

For the preparation of the test specimens, anterior teeth of 2 year old, BSE (spongiform encephalopathy) free cattle were used, which had been slaughtered at a slaughterhouse in Freiburg (Freiburg, Germany). In order to prepare cylinders (diameter: 5 mm, surface area: 19.63 mm², height: 1 mm), as previously described [45], only the buccal surface of the teeth was used. Subsequently, the bovine enamel slabs (BES) were polished by using wet sandpaper in a grinding machine (Knuth-

Rotor-3, Struers, Willich, Germany) in decreasing order of grain size (250 to 4000 grit). The BES were then controlled under a light microscope (Wild M3Z, Leica, Wetzlar, Germany) and were finally disinfected. The BES disinfection protocol involved ultrasonication in NaOCl (3%) for 3 minutes to remove the superficial smear layer, air-drying, and ultrasonication for 3 minutes in 70% ethanol. Finally, the BES were ultrasonicated again for 10 minutes in double-distilled water and stored in distilled water for 24 h to hydrate prior to the assays [46].

Individual maxillary acrylic devices were prepared for each volunteer in the study and six BES were attached approximally using an A-silicon compound (Panasil initial contact X-Light, Kettenbach, Eschenburg, Germany) [47]. The lateral BES margins were covered with silicon to ensure the exposure solely of the BES surfaces in the oral cavity (Fig. 2). With the help of the acrylic appliances the BES were placed at the interdental area between upper premolars and molars, to avoid disturbing movements of the tongue or cheek. Each participant carried twelve BES within the given time periods (2 h, 3 d). To avoid any biofilm disruption, the maxillary splint was not brushed. During meals and the performance of oral hygiene the BES-containing splints were removed and deposited in sterile 0.9% NaCl. The BES were removed from the oral cavity and rinsed with sterile 0.9% saline solution for 30 seconds after the given test periods of 2 h and 3 d, respectively. The silicon was detached from the samples by using sterile tweezers.

Antimicrobial photodynamic therapy (aPDT) of bacterial strains and biofilm samples

Bacterial suspension with different concentrations of ICG (50 µg/ml to 500 µg/ml) were prepared in duplicate in two multiwell plates (24-well plate, Greiner bio-one, Frickenhausen, Germany), with samples containing 1 ml. Negative controls were bacterial strains with 0.9% NaCl, while positive controls were bacterial strains with 0.2% CHX. Prior to irradiation, the multiwell plates were initially incubated for 2 minutes in the dark. Irradiation was then applied to one of the multiwell plates at 37°C for 5 minutes in a water bath while the other plate was further stored in the dark. Each of the experiments was conducted twice. After VIS+wIRA irradiation of *S. mutans, E. faecalis* and *E. corrodens*, a dilution series of each of the treated bacterial solutions was prepared and each dilution was plated on CBA- or HCB plates followed

by cultivation at 37°C in an aerobic atmosphere of 5% CO_2. For *F. nucleatum* and *V. parvula* HCB plates were used to determine the surviving colony forming units (CFU) under anaerobic conditions (anaerobic jars, GENbox anaer, Biomerieux Marcy l'Etoile-France). The procedure as described above applies in principle for the biofilm samples and the human saliva samples. Two out of a total of six specimens were used as controls, one plate served as a negative control treated with NaCl and one plate as a positive control treated with CHX. The remaining samples were treated using aPDT with 300 µg/ml or 450 µg/ml ICG *ex vivo*, respectively. For the application of aPDT, the BES and their adherent biofilms were transferred into a multiwell plate with 1 ml 0.9% NaCl, incubated and then irradiated in the same way as described for the bacterial strains (Fig. 3). Afterwards, the surviving bacteria were plated on CBA- or HCB plates and incubated under both aerobic and anaerobic conditions as described above. Quantification of the microorganisms by determination of the CFU followed. The latter is assumed to have a toxic effect on initially adherent microorganisms and resistant structures, such as oral biofilms. Any heat effect due to radiation from the light source can be excluded by the use of VIS + wIRA.

Live/dead staining and confocal laser scanning microscopy (CLSM)

To quantify the live and dead bacteria within the biofilm, additional BES adherent biofilm samples from a second cycle were obtained for each time period and visualized after appropriate treatment using live/dead staining. For the vital staining and CLSM assay, SYTO 9 and propidium iodide (PI) were used for fluorescent staining (Live/Dead BacLight bacterial viability kit, Life Technologies, Darmstadt, Germany) [48]. The green fluorescent stain can penetrate both intact and damaged bacterial membranes, the red fluorescent staining is only able to penetrate the latter. Therefore, viable bacteria in the CLSM have green fluorescence whereas dead bacteria have red fluorescence. For biofilm staining, the BES were transferred to a multiwell plate, which was filled with 1 ml of SYTO 9 / PI in 0.9% NaCl per well and incubated for 10 minutes at room temperature in the dark. For this purpose, the fluorescent agents were previously diluted with 0.9% NaCl to a final concentration of 0.1 nmol/ml. Following this step, the stained BES were placed face down on a chambered cover glass filled with 20 µl 0.9% NaCl (1 µl-Slide 8 well ibiTreat, ibidi, Munich, Germany) and analyzed using either a 63x water immersion objective (HCX

PL APO/bd. BL, 63.0 x 1.2 W, Leica, Mannheim, Germany) of CLSM (Leica TCS SP2 AOBS, Leica, Mannheim, Germany) for mature biofilms (3 d) or using an Axio Observer Z1 (Carl Zeiss Microscopy, Jena, Germany) with a 63x oil immersion objective (Plan-APOCHROMAT, 63.0 x 1.4 Oil, Carl Zeiss Microscopy, Jena, Germany) for initial biofilms (2 h).

For quantification of the viable biofilm after aPDT and in the control groups, the mature biofilm (3 d) was screened at three representative positions. This resulted in a total of 12 biofilm locations per participant in the four BES to be tested. At each of the three biofilm points, upper and lower boundaries were determined to calculate the mean thickness of the biofilm then scanned in the Z direction, resulting in optical sections about 0.5 µm thick, which were taken at 2 µm intervals throughout the biofilm layers. To reduce the risk of spectral overlap, sequential scanning was used. Each optical section was taken as an image of 1024 x 1024 pixels. The zoom factor was set to 1.7x, corresponding to physical dimensions of 140 by 140 µm per image. In order to increase the number of results in the quantification of viable initial biofilms (2 h) after aPDT, five representative locations were screened per BES. Single images were taken which resulted in a total of 30 biofilm locations in the six BES to be tested. In order to reduce stray fluorescence signal arising from out-of-focus light, an Apotome.2 system (Carl Zeiss Microscopy, Jena, Germany) was utilized. By this method, the system created three images using different grid positions placed in the beam path and automatically calculated the optical section so that only the focal plane was detected.

Image analysis

Image analysis of the mature biofilm (3 d) was carried out as described elsewhere [49]. For the evaluation, a maximal projection for each image stack was generated by LSM Image Browser 5 (Zeiss, Oberkochen, Germany) and the covering grades of the scanned biofilm points were quantified. For further biofilm analysis the red and green image stacks were analyzed using MetaMorph 6.3r7 (Molecular Devices Corporation, Sunnyvale, CA, USA) The intensity thresholds were set manually and separately for each channel of the image stack to define the total surface populated by viable and nonviable microorganisms. For the analysis of the initial biofilm (2 h), which consisted of single images per position, the program ImageJ 1.50i (Wayne Rasband, National Institutes of Health, USA) was used to evaluate the number of pixels in the red-green

projection. After manually setting the threshold, the number of pixels for live and dead bacteria could be counted and the ratio of viable to nonviable microorganisms was determined. The statistical significance of the resulting covering grades (in %) of living and dead cells within the biofilm region was investigated.

Statistical analysis

For descriptive analysis the mean and standard deviation were computed. To compare subgroups linear mixed models with random intercepts for each probing and participant as clusters were applied. For correction of the multiple testing problem (adjustment of p-values), Bonferroni test was used. A Friedman test was used to show differences between the groups in cases of strict not normally distributed data. The statistical analysis was done with STATA 14.2.

Results

APDT in combination with ICG significantly reduces the number of different oral pathogenic microorganisms.

Figures 4A and 4B show the eradication rates of *S. mutans* and *E. corrodens* after application of aPDT using ICG in combination with VIS+wIRA, as well as the untreated negative control and positive control with CHX. APDT showed a significant elimination ($p < 0.001$) of *S. mutans* (4 $\log_{10}$ CFU), already at a concentration of 50 µg/ml ICG, which corresponds to an eradication rate of 99.99%. In the case of *E. corrodens*, significant eradication ($p = 0.002$) of 4 $\log_{10}$ CFU was achieved only at a concentration of 150 µg/ml ICG compared to the untreated negative control. A high killing effect was also shown for the anaerobic bacteria *F. nucleatum* (Fig. 4C) and *V. parvula* (Fig. 4D) at an ICG concentration of 150 µg/ml ($p<0.001$, $p=0.002$). The bacterial count was reduced by a level of 2.7 $\log_{10}$ CFU for *F. nucleatum* and 1.9 $\log_{10}$ CFU for *V. parvula*, which corresponds to a reduction rate of ≥ 98%. Using higher ICG concentrations of 300 µg/ml a reduction up to 99.99% for *F. nucleatum* and 99.9% for *V. parvula* was achieved. In the case of *E. faecalis* shown in Figure 4E, a smaller, yet significant reduction of < 90% in the number of CFU at a concentration of 300 µg/ml ICG was observed ($p<0.001$). However, a higher

eradication of more than 99% (2.4 $\log_{10}$ CFU) was possible at increased concentrations of 500 µg/ml ICG ($p<0.001$). No cultivable bacteria (0 $\log_{10}$ CFU) were detected after treatment with CHX.

ICG with VIS+wIRA significantly reduced the number of planktonic microorganisms within human saliva.

Figures 5A and 5B illustrate the rate of elimination of salivary microorganisms after treatment with and without aPDT and in the control groups. Regarding the untreated negative control, the use of VIS+wIRA (6.9-7.0 $\log_{10}$ CFU) on its own has no appreciable effect on the number of salivary bacteria compared to that of the negative control without aPDT (7.0 $\log_{10}$ CFU). Furthermore, the use of 300 µg/ml ICG without aPDT has no major influence on the number of aerobic or anaerobic microorganisms (6.9-7.0 $\log_{10}$ CFU). In contrast, the combination of ICG and VIS+wIRA led to significant eradication ($p<0.05$) of up to 3 $\log_{10}$ CFU of aerobic bacteria, as well as to a significant reduction ($p<0.05$) of up to 3 $\log_{10}$ CFU of anaerobic microorganisms, signifying a killing rate of 99.9%. In the positive control using 0.2% CHX no bacteria could be detected (0 $\log_{10}$ CFU).

APDT combined with ICG significantly decreased the viable counts of oral microorganisms within initial adhesion and mature biofilm.

Figures 6A and 6B show the eradication of microorganisms from the initial biofilm after 2 h of formation. The control groups are an untreated negative control with a mean value of about 4.5 $\log_{10}$ CFU and a CHX-treated positive control with a mean value of about 0.4 CFU on a $\log_{10}$ scale. Apart from the significant reduction ($p<0.001$) by CHX, aPDT in combination with 300 µg/ml ICG also showed a significant elimination ($p<0.001$) of living aerobic (1.1 $\log_{10}$ CFU) and anaerobic (0.7 $\log_{10}$ CFU) microorganisms. Higher concentrations such as 450 µg/ml ICG with VIS+wIRA led to a complete eradication of the bacteria within the initial biofilm ($p<0.001$), so that no microorganisms could be detected (0 $\log_{10}$ CFU). Figures 6C and 6D show that the number of microorganisms in the untreated mature biofilm of aerobic bacteria was 6.9 $\log_{10}$ CFU and the anaerobic bacteria 7.3 $\log_{10}$ CFU, respectively. Although CHX was used as a positive control it shows a reduction to a mean value of 5.4-5.5 $\log_{10}$ CFU, corresponding to a significant reduction similar to

that seen with the use of aPDT and 300 µg/ml ICG (5.5-5.9 log_{10} CFU). A higher elimination of the viable microorganisms to a mean value of 4.4-4.6 log_{10} CFU was achieved only with the use of aPDT and 450 µg/ml, and corresponds to an eradication rate of oral microorganisms more than 99%.

Live/dead assays showed a high bactericidal effect for aPDT in combination with ICG against oral biofilms.

The quantitative results of the surviving microorganisms after application of VIS+wIRA with ICG, as well as for the CHX-treated positive control and the untreated negative control are illustrated in Figure 7 after formation periods of 2 h and 3 d in boxplots. While 99% of the bacteria that cover the specimen at the initial adhesion in Figure 7A are viable in the untreated control, the statistical analysis revealed a substantial difference ($p<0.001$) in the percentage of vital bacteria in biofilms treated with CHX (3%) or with ICG-mediated aPDT (6%). The results with mature biofilm depicted in Figure 7B showed similar significant differences ($p<0.001$) in the amount of vital bacteria remaining in the positive control with CHX (27%), as well as in the groups treated with aPDT combined with 300 µg/ml (26%) or 450 µg/ml (8%) ICG as compared to the untreated control (82%). In fact, in the presence of 450 µg/ml ICG, significantly more microorganisms were killed within the biofilm ($p<0.001$) compared to lower ICG-concentrations, or compared to the treatment with CHX. The percentages presented above are all median values. Figure 8 shows representative live/dead-CLSM images of aPDT-treated initial biofilm (2 h) using VIS+wIRA and ICG as a photosensitizer. Concerning the untreated control in Figure 8A, isolated dense accumulations of viable bacteria (green) and very few nonviable cells (red) on the BES were detected. In contrast to the dense spatial structures of initially formed biofilm in the negative controls, the composite of the microorganisms after using VIS+wIRA with ICG (Fig. 8B) or treatment with CHX (Fig. 8C) appeared resolved. In addition to the rather homogenous distribution, which is probably due to the detachment of non-viable cells, aPDT as well as CHX caused cell death of the majority of the attached bacteria.

CLSM images show a high penetration of ICG using aPDT within the mature biofilm.

Figure 9 displays representative cross-sectional live/dead-CLSM images of aPDT-treated mature biofilm (3 d) using VIS+wIRA and ICG as a photosensitizer. Examination of the optical sections of the untreated biofilm (negative control) reveals dense organized structures of viable bacteria (green) in different configurations (Figure 9A). The mature biofilm shown in Figure 9B appears after treatment with CHX (positive control) differently. Noticeable is a massive loss of cell viability, as depicted by numerous red-stained bacteria. However, many vital microorganisms remain within deeper layers of the biofilm, suggesting a limited ability of chlorhexidine to penetrate it. The biofilms treated with aPDT and either 300 µg/ml ICG (Figure 9C) or 450 µg/ml ICG (Figure 9D) showed a great amount of dead bacterial cells but without any differences regarding biofilm thickness. After visual observation of the CLSM Z-section galleries the presence of a varied biofilm permeability, dependent on the concentration of the photosensitizer was confirmed (Figures 9C and 9D). More specifically, the oral biofilm appeared more effectively penetrated at a concentration of 450 µg/ml ICG than at 300 µg/ml ICG, as seen from the decreasing number of viable microorganisms in the cross-sectional images after exposure to VIS+wIRA.

Discussion

The present report underlines the effectivesness of an innovative antimicrobial photodynamic approach using aPDT with VIS+wIRA in combination with ICG to treat oral pathogenic bacteria, as well as *in situ*-formed initial and mature oral biofilms. ICG was originally used in the medical field as a diagnostic tool for the study of liver function, ophthalmology and dermatology [50]. Following application to the tissue, the dye is almost completely bound to globulins (80%) and albumin (20%), thereby remaining predominantly intravascular and evenly distributed throughout the circulating blood [51]. Its exclusive elimination via the liver prevents accumulation in the body, making ICG non-toxic and well-tolerated [52]. Side effects are rare and those that appear are possibly due to the 5% sodium iodide contained in the preparation to improve the lessening [11]. Severe side effects have only been described in isolated instances. These include anaphylactic shock, hypotension, tachycardia, dyspnea and urticaria [53]. Due to fluorescent properties in the near infrared range, this provides new possibilities, especially in the field of oncology, to

460 detect tumors for example, or to eliminate malignant tissue under irradiation due to
461 the formation of ROS and the hyperthermia effect, respectively [54].

462 ICG has been recently added, especially for prophylactic use in the field of dentistry,
463 to dyes such as MB and TB, which have successfully been used in the application of
464 aPDT [2,55]. In addition to prevention, photodynamic disinfection in the field of oral
465 surgery and implantology for the sterilization of bone cavities is also possible [14].
466 This non-invasive form of therapy with photosensitizers like MB and TB involves light-
467 induced athermal inactivation of microorganisms without destruction of the
468 surrounding tissue on the basis of light-absorbing dyes, which via release of an
469 oxygen radical, either singlet or triplet oxygen, leads to an oxidizing effect on the
470 bacterial membrane and thus its irreversible damage [29]. In case of ICG, most of the
471 absorbed light is released in the form of heat, so that a predominantly photothermal
472 effect in combination with a photodynamic effect is described [56,57]. In this context,
473 tissue damage by heat is possible, so the laser energy and treatment time must be
474 adjusted. In contrast to other photosensitizers, the reaction with ICG is more specific
475 and safer. The combination of PDT (photodynamic) / PTT (photothermic) by using
476 ICG applications enables saving tissue, as well as sterilization and improved healing
477 [29]. There is still a controversial debate in the case of ICG as to whether the
478 photooxidative effect contributes directly to the therapy or just to the photothermal
479 effect [29]. Whether and how important the influence of the photooxidative effect
480 actually is still needs to be further investigated. However, thermal effects such as
481 overheating and unspecific reactions generated by the light source itself (e.g. by
482 diode laser) can be eliminated by using VIS+wIRA [58].

483 The innovation of this study is the application of different concentrations of ICG to a
484 broad spectrum of bacteria using VIS+wIRA as a light source. Technically, a halogen
485 lamp can generate VIS+wIRA, a broad-band heat radiation with unpolarized light
486 emission ranging between 570 and 1400 nm [22]. After radiation enters the water
487 filter, harmful infrared B and C radiation is absorbed, and the remaining infrared A
488 radiation can pass through deeper tissues at low thermal stress [59]. For a long time
489 the use of VIS+wIRA was limited primarily to the field of dermatology where it has
490 been used against skin tumors, wounds and pain [60,61]. The further introduction
491 into the microbiology for the photoinactivation of diverse pathogens can be related to
492 the high antimicrobial effectiveness of VIS+wIRA [25]. In order to focus on the

proportion of emitted radiation which is infrared A (wIRA; in the range of 780 to 1400 nm), an accessory orange filter (within the range of 570 to 780 nm) can be added to the visible light source [62]. The high energy of the radiation leads to an increase in the metabolic rate. This in turn produces a greater amount of oxygen transferred to deeper tissue layers, while at the same time avoiding thermal stress on the tissue surface [63]. Consistent with our findings from *in vitro*-experiments, another study has found that the possible slight increase in temperature due to VIS+wIRA in the absence of a photosensitizer does not seem to cause any appreciable cell destruction [63]. Although comparable LED devices are low in cost, their emission wavelength spectrum is often quite limited and their use as a light source can lead to tissue overheating [63]. Furthermore, radiators emitting VIS+wIRA are less painful than LED devices and safe when applied at different treatment doses up to 30 minutes [41,64,65]. However, in the present study the treatment duration of 5 minutes proved effective, which also seems realistic for its application in the dental practice.

Significant reduction of selected bacteria that are commonly found in the oral cavity is only be accomplished when aPDT is combined with bacterial-specific concentrations of ICG. In these cases eradication rates of up to 99.99% can be reached, as shown by the present results (Fig. 4). The complete elimination of some bacteria associated with periodontitis, such as *F. nucleatum*, using aPDT with ICG could be demonstrated in the present study at ICG-concentrations of 300 µg/ml and showed results similar to those in a study by Kranz *et al*. [66].The authors examined the influence of Trolox™, a Vitamin E analogue, during aPDT with ICG and Near-IR-laser (810 nm, NIR) on periodontal pathogens. High concentrations of ICG (500 µg/ml) without Trolox™ eliminated *F. nucleatum* and *Porphyromonas gingivalis* completely while temperatures of over 59°C were measured, whereas the addition of 2 mM vitamin E analogue eliminated these germs completely already with lower ICG-concentrations (250 µg/ml) and temperatures of about 50°C. The authors concluded that the combination of ICG and a vitamin E analogue in aPDT reduces the damaging photothermal impact and favors the photooxidative effect [38]. Considering that the NIR light source used by Kranz *et al.* [38] also led to an additional thermal effect, the results with ICG/ Trolox™ are comparable with our results using VIS+wIRA. Furthermore, with the use of ICG we were also able to detect complete elimination of *S. mutans*, one microorganism associated with caries development, as confirmed in another *in vitro* study [67]. Azizi *et al*. [67] examined MB (2%) with ICG

(0.2%= 200 µg/ml) as a photosensitizer in aPDT against *S. mutans* contaminated molars. A diode laser (660 nm and 810 nm, respectively) was used as the light source. The authors showed that after irradiating for 60 seconds and then incubating for 24 h a complete elimination of bacteria could be detected as determined by CFU. In this study we used different concentrations of ICG compared to those used by Azizi *et al.* [67]. At ICG-concentrations of 50 µg/ml a total elimination of *S. mutans* was measured. In an *in vitro* study Beltes *et al*. [32] examined how the growth of a planktonic *E. faecalis* strain was inhibited by NIR irradiation in combination with ICG, with regard to endodontic infections. The ICG-concentration used was 100 µg/ml. The evaluation showed that all approaches to irradiation (different fluence rates and energy doses) and ICG showed significant reduction in bacteria of between approximately 5.1-5.3 $\log_{10}$ in viable counts, whereas when the treatment was with laser or photosensitizer alone there was no reduction of *E. faecalis*. In the present study the growth of *E. faecalis* was significantly reduced (2.3 $\log_{10}$) with VIS+wIRA when combined with ICG at concentrations of 500 µg/ml, with a killing effect of more than 99.9%. Furthermore, aPDT with ICG at a concentration of 150 µg/ml also significantly eliminated *E. corrodens* (99.99%) and significantly reduced *V. parvula* (>99.9%). This could be caused by the Gram-negative cell wall of *V. parvula*, which may lead to low permeability of ICG. Our results obtained with VIS+wIRA on planktonic bacteria showed the antimicrobial effect was dependent on the ICG concentration used Topaloglu *et al.* [68] reported on the risk that lower ICG concentrations used during aPDT can not only eliminate bacteria but actually increase the proliferation rate of bacteria, as demonstrated in *in vitro* experiments with *Pseudomonas aeruginosa* [30]. This was explained by the amount of reactive oxygen species, which was generated and determines the actual level of bactericidal effect or proliferation.

In addition to the positive properties of aPDT when combined with ICG already mentioned, there are further advantages in the dental field, as described by Meisel and Kocher [71]. These include a possible eradication of bacteria in hard-to-reach niches such as tooth pockets in the case of periodontitis [72] or the surfaces of implants [73]. Mechanical treatments for biofilm removal lead to increased dentin sensitivity, and could then be omitted. Furthermore, the risk of bacteremia and periodontal systemic diseases such as heart disease and diabetes could be reduced.

Naturally occurring biofilms are usually made up of a network of strains from a broad spectrum of bacteria rather than a single strain. To more closely approach this condition saliva was obtained from healthy study participants and also applied with VIS+wIRA in combination with ICG. These experiments also showed a significant reduction in bacteria, roughly correlating with an eradication rate of 99.99%. In contrast, the use of either VIS+wIRA or ICG on their own showed no bacterial reduction. However, one must consider that microorganisms living in biofilms are up to 1000 times more resistant to antimicrobials than their planktonic counterparts [74]. For this reason, our present investigation into the effect of aPDT in combination with ICG on *in situ* formed biofilms seemed reasonable.

To the best of our knowledge this is the first time that aPDT with VIS+wIRA in combination with the photosensitizer ICG have been used to treat *in situ* oral biofilms. Most publications dealing with the antimicrobial effects of aPDT using ICG are conducting their studies on planktonic cultures, with only a few investigating its use on bacterial biofilms. However, it must be taken into account that until now, the results regarding aPDT in combination with ICG were obtained using a diode laser as a light source and that possible tissue damage due to the thermal effect cannot be excluded. Since the killing effect of microorganisms within the mature oral biofilm was limited to 3 log, repeated treatments are recommended to overcome the doubling time of bacteria which could be less than one hour. Nevertheless, such killing rates would have destroyed the balance of the mature oral biofilm, as has been shown in detail in our earlier study [40]

The use of bovine enamel as performed in the present study simulates a bacterial attachment to human enamel as it has common physicochemical features with human tooth surfaces. The use of artificial tooth substrata was avoided due to the altered biofilm composition compared to that on natural tooth surfaces [75]. Quantification of CFU after irradiation of the oral biofilm showed a significant reduction at the concentrations of ICG tested, with a correlation between the amount of photosensitizer and the rate of eradication. Furthermore, it was demonstrated that an ICG-based aPDT had an erosive effect on the carious hard tissue, depending on laser irradiation and the concentration of the dye [76,77]. Beltes *et al*. [32] examined the effect of ICG under NIR irradiation to *E. faecalis* in infected root canals *ex vivo*. The authors found that aPDT using NIR in combination with 100 µg/ml ICG reduced

593 the *E. faecalis* viable count by a level of 99.99% (4 $\log_{10}$ CFU). However, the
594 bacterial culture in the infected root canals was 72 h old compared to the *E. faecalis*
595 culture treated overnight in the present study.

596 Beytollahi *et al.* [34] compared the effects of ICG versus TB combined with a diode
597 laser on the formation of biofilm in *S. mutans*. The authors found that increasing
598 photosensitizer concentrations resulted in a reduction in biofilm formation. The
599 maximum level of reduction was at 1 mg/ml ICG and 0.1 mg/ml TB. At the same time,
600 a change in cell morphology was observed in the aPDT-treated cells compared to the
601 untreated cells, along with the formation of an irregular-looking biofilm and a loss of
602 cell interaction, which was also confirmed by our live/dead staining results. A different
603 approach was presented by a study investigating the influence of sub-lethal doses of
604 various photosensitizers and diode laser irradiation on biofilm formation of the
605 endodontic bacterium *E. faecalis* [29]. It was shown that ICG-concentrations of 31.2
606 µg/ml up to 1000 µg/ml without irradiation were able to significantly, although not
607 completely, inhibit bacterial growth. With irradiation, the survival rate was dependent
608 on the light dose. The authors revealed that sub-lethal doses have an inhibitory effect
609 on bacterial physiology, and that the low dose of ICG tested reduced the bacterial
610 biofilm by 42.8%, more than MB and TB, which each showed a reduction less than
611 20%. Because a further decrease in the sub-lethal concentration can actually
612 improve biofilm formation [69], the optimal dose must be determined before
613 application. In the present study, the live/dead staining images illustrate, in addition
614 to majority of the microorganisms dying, there was a change of the dense biofilm
615 upon treatment with VIS+wIRA and ICG compared to the untreated control, indicating
616 an aPDT-induced alteration in biofilm architecture. Chiniforush *et al.* [78] already
617 mentioned the possible influence on bacterial behavior through the alteration of
618 virulence factors when aPDT is used in combination with ICG, which could in turn
619 also influence biofilm topography. Interestingly, the CLSM images presented in this
620 study visualized viable and nonviable organisms and showed a limited depth of
621 penetration for CHX. These studies also showed that bacteria in deeper layers of the
622 mature biofilm were killed when irradiation was combined with ICG, emphasizing its
623 high permeability within the oral biofilm in this instance. An investigation of Bashkatov
624 *et al.* [79] has shown that near-infrared light, as used in the aPDT with ICG (810 nm),
625 penetrates up to 6 mm into the tissue while wavelengths in the range of 650 nm,
626 used with other photosensitizers, only penetrate to a depth of 3-3.5 mm. Therefore,

the depth effect of VIS+wIRA with ICG is extended compared to other established photosensitizers because microorganisms in the adjacent area are also reached.

Conclusions & Future perspective

In conclusion, due to the recent increase in antibiotic resistance alternative therapies such as aPDT, with its benefits that already resistant bacteria can be eliminated while no resistance to the treatment can be developed, are now a focus of research. The results of the present study with aPDT in combination with ICG and using VIS+wIRA as a light source demonstrated that not only planktonic bacteria or bacteria in saliva but also initial and mature biofilm can be effectively eliminated. These findings indicate that this method could be established as an alternative to chemical and antibiotic treatments, especially in the field of dentistry. Compared to other light sources VIS+wIRA is less painful, thermal stress is reduced, and tissue damage is avoided. Further *in situ* investigations should be carried out to assess optimal ICG concentrations for a wide spectrum of oral pathogens, as well as to clarify if the effect of ICG is more photothermal or photooxidative and to examine these effects on the tissue. Taking the healing effects of wIRA on human tissue into consideration, this technique could prove to be helpful in the treatment of oral diseases such as periimplantitis and periodontitis, though its use in dentistry should be evaluated in future clinical trials. An irradiation setup should be developed for clinical use, particularly within the oral cavity. This type of application should be examined in future clinical studies *in vivo*.

Summary Points

- Due to the increase of antibiotic resistance, alternative antimicrobial treatments such as antimicrobial photodynamic therapy (aPDT) are required.
- aPDT using visible light and water-filtered infrared A radiation (VIS+wIRA) in combination with indocyanine green (ICG) was tested against oral pathogenic bacteria, total human salivary bacteria, and the *in situ* initial and mature oral biofilm.

- This novel aPDT strongly reduced the number of different oral pathogenic microorganisms (killing rate ≥ 99.9%).
- The number of planktonic microorganisms within human saliva was significantly reduced by ICG and VIS+wIRA.
- aPDT combined with ICG significantly decreased the viable counts of oral microorganisms within initial adhesion and mature biofilm.
- The aPDT using VIS+wIRA and ICG has the potential to treat periodontitis and peri-implantitis as an adjunct therapy.

References

Papers of special note have been highlighted as: • of interest; •• of considerable interest

1. Nagata JY, Hioka N, Kimura E, *et al.* Antibacterial photodynamic therapy for dental caries: Evaluation of the photosensitizers used and light source properties. *Photodiagnosis Photodyn. Ther.* 9(2), 122–131 (2012).

2. Dascalu (Rusu) ML, Sarosi C, Moldovan M, Badea ME. A Study on Revealing Agents in the Context of Photodynamic Therapy in Dental Medicine - A Literature Review. *Defect Diffus. Forum*. 376, 54–65 (2017).

3. Pourhajibagher M, Bahador A. An in vivo evaluation of microbial diversity before and after the photo-activated disinfection in primary endodontic infections: Traditional phenotypic and molecular approaches. *Photodiagnosis Photodyn. Ther.* 22, 19–25 (2018).

4. Dobson J, Wilson M. Sensitization of oral bacteria in biofilms to killing by light from a low-power laser. *Arch. Oral Biol.* 37(11), 883–887 (1992).

5. Garcez AS, Hamblin MR. Methylene Blue and Hydrogen Peroxide for Photodynamic Inactivation in Root Canal - A New Protocol for Use in Endodontics. *Eur. Endod. J.* 2(1), 29–29 (2017).

6. Narayanan LL, Vaishnavi C. Endodontic microbiology. *J. Conserv. Dent. JCD*. 13(4), 233-239 (2010).

7. Fontana C, Abernethy A, Som S, *et al.* The antibacterial effect of photodynamic therapy in dental plaque-derived biofilms. *J. Periodontal Res.* 44(6), 751–759 (2009).

8. Wood S, Nattress B, Kirkham J, *et al.* An in vitro study of the use of photodynamic therapy for the treatment of natural oral plaque biofilms formed in vivo. *J. Photochem. Photobiol. B*. 50(1), 1–7 (1999).

9. Tavares LJ, Pavarina AC, Vergani CE, de Avila ED. The impact of antimicrobial photodynamic therapy on peri-implant disease: What mechanisms are involved in this novel treatment? *Photodiagnosis Photodyn. Ther.* 17, 236–244 (2017).

10. Jurič IB, Plečko V, Pandurić DG, Anić I. The antimicrobial effectiveness of photodynamic therapy used as an addition to the conventional endodontic re-treatment: A clinical study. *Photodiagnosis Photodyn. Ther.* 11(4), 549–555 (2014).

11. Chiniforush N, Pourhajibagher M, Shahabi S, Bahador A. Clinical Approach of High Technology Techniques for Control and Elimination of Endodontic Microbiota. *J. Lasers Med. Sci.* 6(4), 139–150 (2015).

12. Diogo P, Fernandes C, Caramelo F, *et al.* Antimicrobial photodynamic therapy against endodontic Enterococcus faecalis and Candida albicans mono and mixed biofilms in the presence of photosensitizers: A comparative study with classical endodontic irrigants. *Front. Microbiol.* 8, 498 (2017).

13. Meimandi M, Ardakani MRT, Nejad AE, Yousefnejad P, Saebi K, Tayeed MH. The effect of photodynamic therapy in the treatment of chronic periodontitis: A review of literature. *J. Lasers Med. Sci.* 8(Suppl 1), S7 (2017).

14. Nagayoshi M, Nishihara T, Nakashima K, *et al.* Bactericidal Effects of Diode Laser Irradiation on Enterococcus faecalis Using Periapical Lesion Defect Model. *ISRN Dent.* Vol 2011, 870364 (2011).

15. Faria PEP, Felipucci DNB, Simioni AR, Primo FL, Tedesco AC, Salata LA. Effects of photodynamic process (PDP) in implant osseointegration: a histologic and histometric study in dogs. *Clin. Implant Dent. Relat. Res.* 17(5), 879–890 (2015).

16. Cieplik F, Tabenski L, Buchalla W, Maisch T. Antimicrobial photodynamic therapy for inactivation of biofilms formed by oral key pathogens. *Front. Microbiol.* 5, 405 (2014).

• • Review depicting the use of different photosensitizers and light sources for the antimicrobial photodynamic inactivation of oral pathogens.

17. Araújo TSD, Rodrigues PLF, Santos MS, *et al.* Reduced methicillin-resistant Staphylococcus aureus biofilm formation in bone cavities by photodynamic therapy. *Photodiagnosis Photodyn. Ther.* 21, 219–223 (2018).

18. Azizi B, Budimir A, Bago I, *et al.* Antimicrobial efficacy of photodynamic therapy and light-activated disinfection on contaminated zirconia implants: An in vitro study. *Photodiagnosis Photodyn. Ther.* 21, 328–333 (2018).

19. Decker E-M, Bartha V, von Ohle C. Improvement of Antibacterial Efficacy Through Synergistic Effect in Photodynamic Therapy Based on Thiazinium

730 Chromophores Against Planktonic and Biofilm-Associated Periodontopathogens.
731 *Photomed. Laser Surg.* 35(4), 195–205 (2017).

732 20. Karygianni L, Ruf S, Follo M, *et al.* Novel Broad-Spectrum Antimicrobial
733 Photoinactivation of In Situ Oral Biofilms by Visible Light plus Water-Filtered
734 Infrared A. *Appl. Environ. Microbiol.* 80(23), 7324–7336 (2014).

735 • One of the first articles introducing the aPDT using VIS+wIRA in combination with
736 other photosensitizers

737 21. Hoffmann G, Hartel M, Mercer JB. Heat for wounds - water-filtered infrared-A
738 (wIRA) for wound healing - a review. *Ger. Med. Sci. GMS E-J.* 14, Doc08 (2016).

739 • • Review depicting the different healing effects of wIRA.

740 22. Jung T, Grune T. Experimental basis for discriminating between thermal and
741 athermal effects of water-filtered infrared A irradiation: Thermal and athermal
742 wIRA effects. *Ann. N. Y. Acad. Sci.* 1259, 33–38 (2012).

743 23. Künzli BM, Liebl F, Nuhn P, Schuster T, Friess H, Hartel M. Impact of
744 Preoperative Local Water-Filtered Infrared A Irradiation on Postoperative Wound
745 Healing: A Randomized Patient- and Observer-Blinded Controlled Clinical Trial.
746 *Ann. Surg.* 258(6), 887–894 (2013).

747 24. Hoffmann G. Water-filtered infrared-A (wIRA) in acute and chronic wounds.
748 *GMS Krankenhaushygiene Interdiszip.* 4(2), Doc12 (2009).

749 25. Al-Ahmad A, Tennert C, Karygianni L, Wrbas KT, Hellwig E, Altenburger MJ.
750 Antimicrobial photodynamic therapy using visible light plus water-filtered
751 infrared-A (wIRA). *J. Med. Microbiol.* 62(Pt 3), 467–473 (2013).

752 26. United States Food and Drug Administration. Approval of “IC-Green” [Internet].
753 NDA 011525 (1959). Available from:
754 https://www.accessdata.fda.gov/scripts/cder/daf/index.cfm?event=overview.proc
755 ess&applno=011525.

756 27. Giraudeau C, Moussaron A, Stallivieri A, Mordon S, Frochot C. Indocyanine
757 Green: Photosensitizer or Chromophore? Still a Debate. *Curr. Med. Chem.*
758 21(16), 1871–1897 (2014).

759 • • Review discussing the use of indocyanine green for different treatments

760 28. Reindl S, Penzkofer A, Gong S-H, *et al.* Quantum yield of triplet formation for
761 indocyanine green. *J. Photochem. Photobiol. Chem.* 105, 65–68 (1997).

762 29. Hopp M, Biffar R. Die ICG-gestütze Photothermische Therapie (PTT). *ZMK*.
763 29(9), 528–541 (2013).

764 30. Urbanska K, Romanowska-Dixon B, Matuszak Z, Oszajca J, Nowak-Sliwinska P,
765 Stochel G. Indocyanine green as a prospective sensitizer for photodynamic
766 therapy of melanomas*. *Acta Biochim. Pol.* 49(2), 387–391 (2002).

31. Engelschalk M. Photodynamische Therapie oder Photothermale Therapie. *Laser J.* 16(2), 12–14 (2013).

32. Beltes C, Economides N, Sakkas H, Papadopoulou C, Lambrianidis T. Evaluation of Antimicrobial Photodynamic Therapy Using Indocyanine Green and Near-Infrared Diode Laser Against *Enterococcus faecalis* in Infected Human Root Canals. *Photomed. Laser Surg.* 35(5), 264–269 (2017).

33. Afkhami F, Akbari S, Chiniforush N. Entrococcus faecalis elimination in root canals using silver nanoparticles, photodynamic therapy, diode laser, or laser-activated nanoparticles: an in vitro study. *J. Endod.* 43(2), 279–282 (2017).

34. Beytollahi L, Pourhajibagher M, Chiniforush N, *et al.* The efficacy of photodynamic and photothermal therapy on biofilm formation of Streptococcus mutans : An in vitro study. *Photodiagnosis Photodyn. Ther.* 17, 56–60 (2017).

35. Pourhajibagher M, Chiniforush N, Parker S, *et al.* Evaluation of antimicrobial photodynamic therapy with indocyanine green and curcumin on human gingival fibroblast cells: An in vitro photocytotoxicity investigation. *Photodiagnosis Photodyn. Ther.* 15, 13–18 (2016).

36. Bolhari B, Pourhajibagher M, Bazarjani F, *et al.* Ex vivo assessment of synergic effect of chlorhexidine for enhancing antimicrobial photodynamic therapy efficiency on expression patterns of biofilm-associated genes of Enterococcus faecalis. *Photodiagnosis Photodyn. Ther.* 22, 227–232 (2018).

37. Akbari T, Pourhajibagher M, Hosseini F, *et al.* The effect of indocyanine green loaded on a novel nano-graphene oxide for high performance of photodynamic therapy against Enterococcus faecalis. *Photodiagnosis Photodyn. Ther.* 20, 148–153 (2017).

38. Pourhajibagher M, Chiniforush N, Ghorbanzadeh R, Bahador A. Photo-activated disinfection based on indocyanine green against cell viability and biofilm formation of Porphyromonas gingivalis. *Photodiagnosis Photodyn. Ther.* 17, 61–64 (2017).

39. Omar GS, Wilson M, Nair SP. Lethal photosensitization of wound-associated microbes using indocyanine green and near-infrared light. *BMC Microbiol.* 8, 111 (2008).

40. Al-Ahmad A, Bucher M, Anderson AC, *et al.* Antimicrobial Photoinactivation Using Visible Light Plus Water-Filtered Infrared-A (VIS + wIRA) Alters In Situ Oral Biofilms. *PLoS ONE*. 10(7), e0132107 (2015).

41. Piazena H, Kelleher DK. Effects of Infrared-A Irradiation on Skin: Discrepancies in Published Data Highlight the Need for an Exact Consideration of Physical and Photobiological Laws and Appropriate Experimental Settings. *Photochem. Photobiol.* 86(3), 687–705 (2010).

•• One of the first articles clearly showing the positive effects of IRA on the skin and stressing the need for an appropriate setting

42. Vaupel P, Piazena H, Müller W, Notter M. Biophysical and photobiological basics of water-filtered infrared-A hyperthermia of superficial tumors. *Int. J. Hyperthermia*. 35(1), 26–36 (2018).

43. Piazena H, Meffert H, Uebelhack R. Spectral Remittance and Transmittance of Visible and Infrared-A Radiation in Human Skin-Comparison Between *in vivo* Measurements and Model Calculations. *Photochem. Photobiol.* 93(6), 1449–1461 (2017).

44. Jones D, Pell PA, Sneath PHA. Maintenance of bacteria on glass beads at–60 °C to–76 °C. In: *B. E. Kirsop and J.J.S. Snell (Eds.) Maintenance of Microorganisms: A Manual of Laboratory Methods*, Academic Press, London, UK, 35–40 (1984).

45. Karygianni L, Follo M, Hellwig E, *et al.* Microscope-Based Imaging Platform for Large-Scale Analysis of Oral Biofilms. *Appl. Environ. Microbiol.* 78(24), 8703–8711 (2012).

46. Al-Ahmad A, Follo M, Selzer A-C, Hellwig E, Hannig M, Hannig C. Bacterial colonization of enamel in situ investigated using fluorescence in situ hybridization. *J. Med. Microbiol.* 58(10), 1359–1366 (2009).

47. Al-Ahmad A, Wiedmann-Al-Ahmad M, Fackler A, *et al.* In vivo study of the initial bacterial adhesion on different implant materials. *Arch. Oral Biol.* 58(9), 1139–1147 (2013).

48. Tawakoli PN, Al-Ahmad A, Hoth-Hannig W, Hannig M, Hannig C. Comparison of different live/dead stainings for detection and quantification of adherent microorganisms in the initial oral biofilm. *Clin. Oral Investig.* 17(3), 841–850 (2013).

49. Al-Ahmad A, Wunder A, Auschill TM, *et al.* The in vivo dynamics of Streptococcus spp., Actinomyces naeslundii, Fusobacterium nucleatum and Veillonella spp. in dental plaque biofilm as analysed by five-colour multiplex fluorescence in situ hybridization. *J. Med. Microbiol.* 56(5), 681–687 (2007).

50. Landsman ML, Kwant G, Mook GA, Zijlstra WG. Light-absorbing properties, stability, and spectral stabilization of indocyanine green. *J. Appl. Physiol.* 40(4), 575–583 (1976).

51. Fox IJ, Brooker LGS, Heseltime DW, Wood EH. A new dye for continous recording of dilution curves in whole blood independent of variations in blood oxygen saturation. *Circulation*. 14, 937–938 (1956).

52. Cherrick GR, Stein SW, Leevy CM, Davidson CS. INDOCYANINE GREEN: OBSERVATIONS ON ITS PHYSICAL PROPERTIES, PLASMA DECAY, AND HEPATIC EXTRACTION*. *J. Clin. Invest.* 39(4), 592–600 (1960).

53. Benya R, Quintana J, Brundage B. Adverse reactions to indocyanine green: a case report and a review of the literature. *Cathet. Cardiovasc. Diagn.* 17(4), 231–233 (1989).

54. Porcu EP, Salis A, Gavini E, Rassu G, Maestri M, Giunchedi P. Indocyanine green delivery systems for tumour detection and treatments. *Biotechnol. Adv.* 34(5), 768–789 (2016).

• • Review reporting the use of indocynine green in the oncological field.

55. Bach G. Langzeitbehandlung periimplantärer Läsionen in der Alterszahnheilkunde. *LASER J.* 2013(1), 35–37 (2013).

56. Fekrazad R, Khoei F, Hakimiha N, Bahador A. Photoelimination of Streptococcus mutans with two methods of photodynamic and photothermal therapy. *Photodiagnosis Photodyn. Ther.* 10(4), 626–631 (2013).

57. Engel E, Schraml R, Maisch T, *et al.* Light-Induced Decomposition of Indocyanine Green. *Invest. Ophthalmol. Vis. Sci.* 49(5), 1777–1783 (2008).

58. Al-Ahmad A, Walankiewicz A, Hellwig E, *et al.* Photoinactivation Using Visible Light Plus Water-Filtered Infrared-A (vis+wIRA) and Chlorine e6 (Ce6) Eradicates Planktonic Periodontal Pathogens and Subgingival Biofilms. *Front. Microbiol.* 7, 1900 (2016).

59. Rolim JPML, de-Melo MAS, Guedes SF, *et al.* The antimicrobial activity of photodynamic therapy against Streptococcus mutans using different photosensitizers. *J. Photochem. Photobiol. B*. 106, 40–46 (2012).

60. Akca O, Melischek M, Scheck T, *et al.* Postoperative pain and subcutaneous oxygen tension. *The Lancet*. 354, 41–42 (1999).

61. Hürlimann AF, Hänggi G, Panizzon RG. Photodynamic Therapy of Superficial Basal Cell Carcinomas Using Topical 5-Aminolevulinic Acid in a Nanocolloid Lotion. *Dermatology*. 197, 248–254 (1998).

62. Schumann H, Calow T, Weckesser S, Müller ML, Hoffmann G. Water-filtered infrared A for the treatment of chronic venous stasis ulcers of the lower legs at home: a randomized controlled blinded study: wIRA for chronic venous stasis ulcers. *Br. J. Dermatol.* 165(3), 541–551 (2011).

63. Von Felbert V, Hoffmann G, Hoff-Lesch S, *et al.* Photodynamic therapy of multiple actinic keratoses: reduced pain through use of visible light plus water-filtered infrared A compared with light from light-emitting diodes: PDT of multiple AKs: reduced pain through VIS + wIRA. *Br. J. Dermatol.* 163(3), 607–615 (2010).

• One of the first articles to clearly show the pain reducing effects of VIS+wIRA compared to other widely used light sources

64. Jung T, Höhn A, Piazena H, Grune T. Effects of water-filtered infrared A irradiation on human fibroblasts. *Free Radic. Biol. Med.* 48, 153–160 (2010).

65. Giehl KA, Kriz M, Grahovac M, Ruzicka T, Berking C. A controlled trial of photodynamic therapy of actinic keratosis comparing different red light sources. *Eur. J. Dermatol.* 24(3), 335–341 (2014).

66. Kranz S, Huebsch M, Guellmar A, Voelpel A, Tonndorf-Martini S, Sigusch BW. Antibacterial photodynamic treatment of periodontopathogenic bacteria with indocyanine green and near-infrared laser light enhanced by TroloxTM. *Lasers Surg. Med.* 47(4), 350–360 (2015).

67. Azizi A, Shademan S, Rezai M, Rahimi A, Lawaf S. Effect of photodynamic therapy with two photosensitizers on Streptococcus mutants: In vitro study. *Photodiagnosis Photodyn. Ther.* 16, 66–71 (2016).

68. Topaloglu N, Guney M, Aysan N, Gulsoy M, Yuksel S. The role of reactive oxygen species in the antibacterial photodynamic treatment: photoinactivation *vs* proliferation. *Lett. Appl. Microbiol.* 62(3), 230–236 (2016).

69. Pourhajibagher M, Chiniforush N, Shahabi S, Ghorbanzadeh R, Bahador A. Sub-lethal doses of photodynamic therapy affect biofilm formation ability and metabolic activity of Enterococcus faecalis. *Photodiagnosis Photodyn. Ther.* 15, 159–166 (2016).

70. Topaloglu N, Gulsoy M, Yuksel S. Antimicrobial Photodynamic Therapy of Resistant Bacterial Strains by Indocyanine Green and 809-nm Diode Laser. *Photomed. Laser Surg.* 31(4), 155–162 (2013).

• An article demonstrating the antimicrobial effects of indocynine green agains both Gram-negative and Gram-positive bacteria.

71. Meisel P, Kocher T. Photodynamische Therapie in der Parodontologie Viele Studien, wenig Evidenz. Gemeinsame wissenschaftliche Mitteilung der Deutschen Gesellschaft für Parodontologie und der Gesellschaft für Zahn-Mund- und Kieferheilkunde. *Parodontologie*. 48, 591–599 (2015).

72. Srikanth K, Chandra RV, Reddy AA, Reddy BH, Reddy C, Naveen A. Effect of a single session of antimicrobial photodynamic therapy using indocyanine green in the treatment of chronic periodontitis: A randomized controlled pilot trial. *Quintessence Int.* 46(5), 391–400 (2015).

73. Saffarpour A, Fekrazad R, Heibati M, *et al.* Bactericidal Effect of Erbium-Doped Yttrium Aluminum Garnet Laser and Photodynamic Therapy on Aggregatibacter Actinomycetemcomitans Biofilm on Implant Surface. *Int. J. Oral Maxillofac. Implants*. 31(3), e71–e78 (2016).

74. Chambless JD, Hunt SM, Stewart PS. A Three-Dimensional Computer Model of Four Hypothetical Mechanisms Protecting Biofilms from Antimicrobials. *Appl. Environ. Microbiol.* 72(3), 2005–2013 (2006).

75. Teles FR, Teles RP, Sachdeo A, *et al.* Comparison of Microbial Changes in Early Redeveloping Biofilms on Natural Teeth and Dentures. *J. Periodontol.* 83(9), 1139–1148 (2012).

76. De Sant'anna GR, Dos Santos EAP, Soares LES, *et al.* Dental Enamel Irradiated with Infrared Diode Laser and Photoabsorbing Cream: Part 1—FT-Raman Study. *Photomed. Laser Surg.* 27(3), 499–507 (2009).

77. McNally KM, Gillings BRD, Dawes JM. Dye-assisted diode laser ablation of carious enamel and dentine. *Aust. Dent. J.* 44(3), 169–175 (1999).

78. Chiniforush N, Pourhajibagher M, Shahabi S, Kosarieh E, Bahador A. Can Antimicrobial Photodynamic Therapy (aPDT) Enhance the Endodontic Treatment? *J. Lasers Med. Sci.* 7(2), 76–85 (2016).

79. Bashkatov AN, Genina EA, Kochubey VI, Tuchin VV. Optical properties of human skin, subcutaneous and mucous tissues in the wavelength range from 400 to 2000 nm. *J. Phys. Appl. Phys.* 38(15), 2543–2555 (2005).

Figures and boxes

FIG 1: Absorption spectrum of the indocyanine green in water. The concentration of the dye was 300 µg/ml. The measurement of the spectrum was conducted a Tecan Infinite 200 reader (Tecan, Crailsheim, Germany).

FIG 2: Individual acrylic splints with six enamel slabs attached to different locations. The slabs were placed in the front (f), in the middle (m) and in the back (b) on both sides, right (R) and left (L). All sides of the slabs except the enamel surface were covered with silicone and embedded in the appliance.

FIG 3: Schematic representation aPDT with visible light (VIS) plus water-filtered infrared A (wIRA). The tested photosensitizer indocyanine green (ICG) reached an excited singlet state after the application of a broadband VIS + wIRA radiator with a water-filtered spectrum ranging between 570 and 1400 nm. The excited photosensitizer interacted with oxygen (O_2), resulting to the release of thermal energy and various reactive oxygen species (ROS).

FIG 4: Graphs of the numbers of CFU showing photodynamic efficacy against various periodontal pathogens previously grown as overnight cultures *in vitro*. The concentrations of the used photosensitizer indocyanine green (ICG), an untreated negative control and a CHX-treated positive control are shown both with and without the use of aPDT. The CFU are displayed on a $\log_{10}$ scale per milliliter ($\log_{10}$ CFU/ml). All significant p-values are marked on the graphs.

FIG 5: Diagrams of the reduction of planktonic microorganisms in total human saliva after use of indocyanine green (ICG) in combination with and in the absence of VIS+wIRA. In addition to the untreated negative control and the 0.2% chlorhexidine-treated positive control, the concentration of 300 µg/ml ICG used was determined based on earlier *in vitro* experiments. The CFUs are presented on a $\log_{10}$ scale per milliliter ($\log_{10}$ CFU/ml).

FIG 6: Plots of eradication rates of initially formed biofilms (2 h) and mature biofilms (3 d) after use of aPDT in combination with ICG. The control groups are an untreated negative control and a 0.2% chlorhexidine-treated positive control. The number of

CFUs is presented on a log_{10} scale per square centimeter (log_{10} CFU/cm²). The significant p-values are marked in the diagrams.

FIG 7: Boxplots depicting percentages of the live bacterial cells following live/dead staining after 2 h (initial adhesion) and 3 d (mature biofilm), and aPDT with ICG as a photosensitizer. The untreated negative control and 0.2% CHX-treated positive control were also tested. The whiskers indicate minimum and maximum, while the median is represented by the internal line in each box. The significant p-values are provided.

FIG 8: Widefield live/dead images demonstrating the effect of aPDT on initially formed biofilm (2h. Illustrated are live (green) and dead (red) bacterial cells within the untreated negative control (A), CHX-treated positive control (B), and aPDT-treated biofilms after using ICG (C) in the presence of VIS+wIRA. Each image displays maximum projections of the examined surface area.

FIG 9: Z-section galleries of representative live/dead-CLSM images of aPDT-treated mature biofilms (3 days). The panels illustrate the live (green) and dead (red) bacterial cells of the untreated negative control (A), CHX-treated positive control (CHX) (B), and aPDT-treated biofilms in the presence of either 300 µg/ml indocyanine green (ICG) (C) or 450 µg/ml indocyanine green (ICG) (D). Vertical sectioning was used to generate multiple Z-sections at 2 µm intervals through the sample above the surface, respectively. Scale bars represent a length of 10 µm.

FIG 1

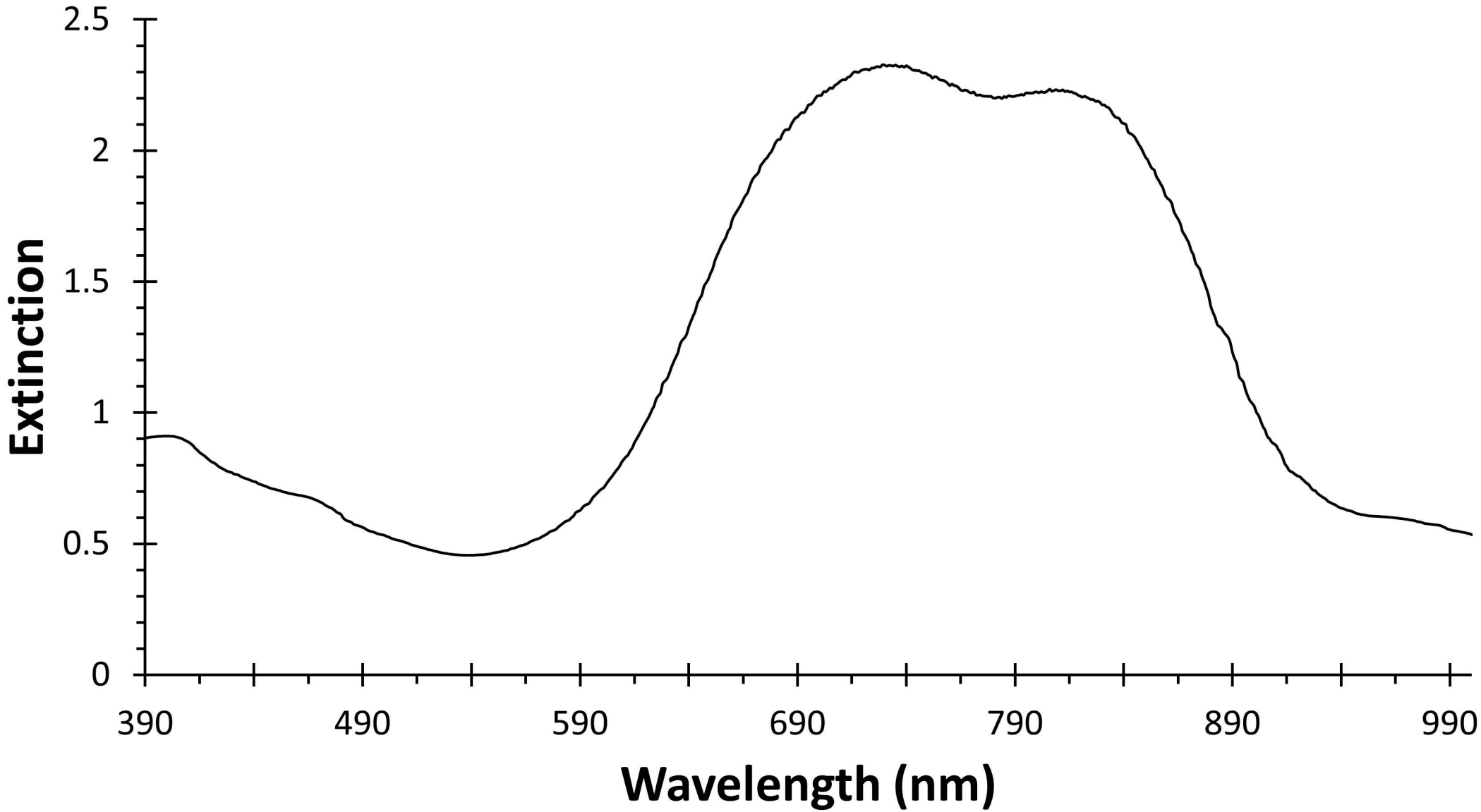
2.5
2
1.5
1
0.5
0
Extinction
390
490
590
690
790
890
990
Wavelength (nm)

FIG 2

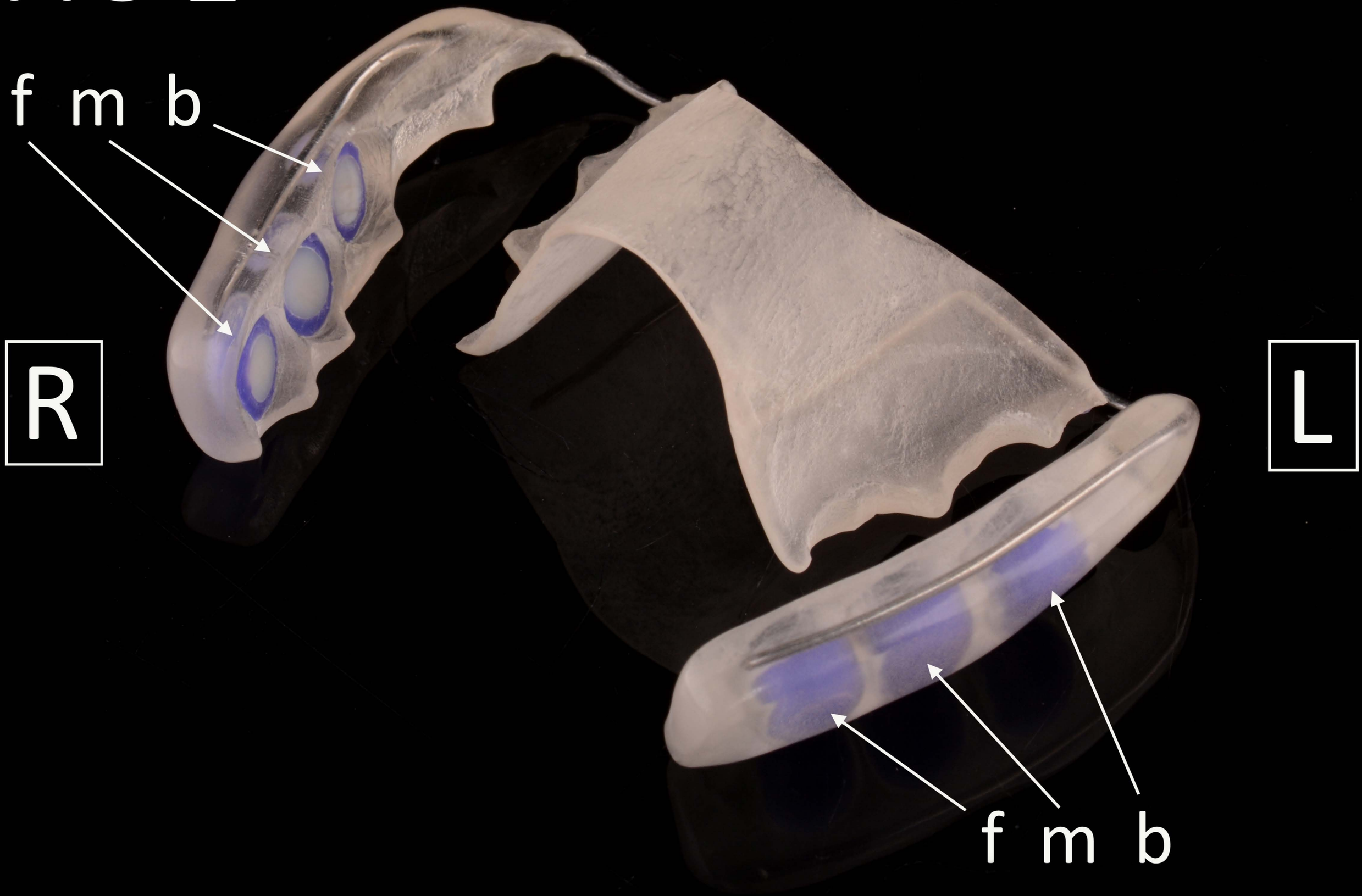

FIG 3

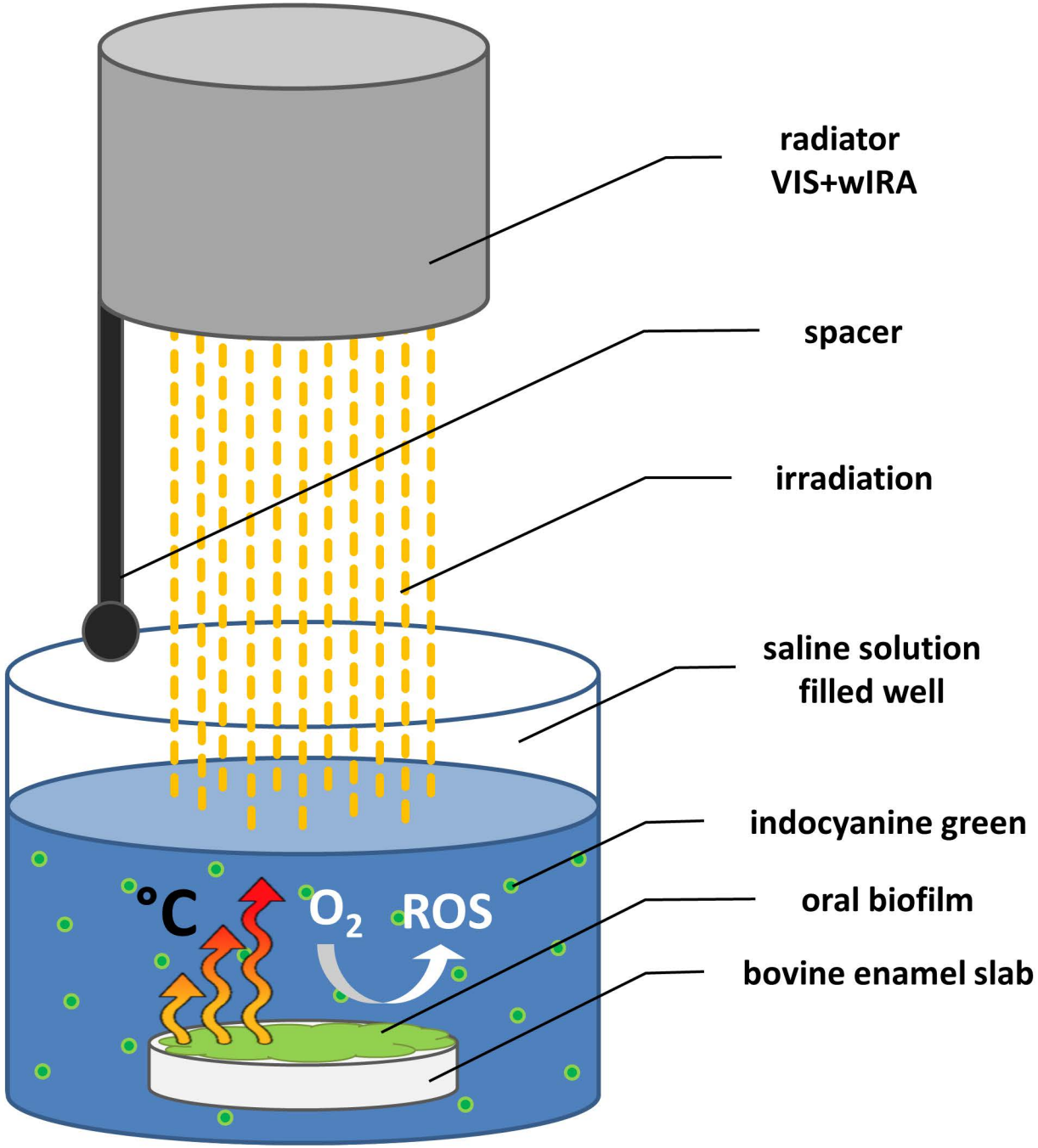
radiator
VIS+wIRA
spacer
irradiation
saline solution
filled well
indocyanine green
oral biofilm
bovine enamel slab
°C
O_2
ROS

FIG 4

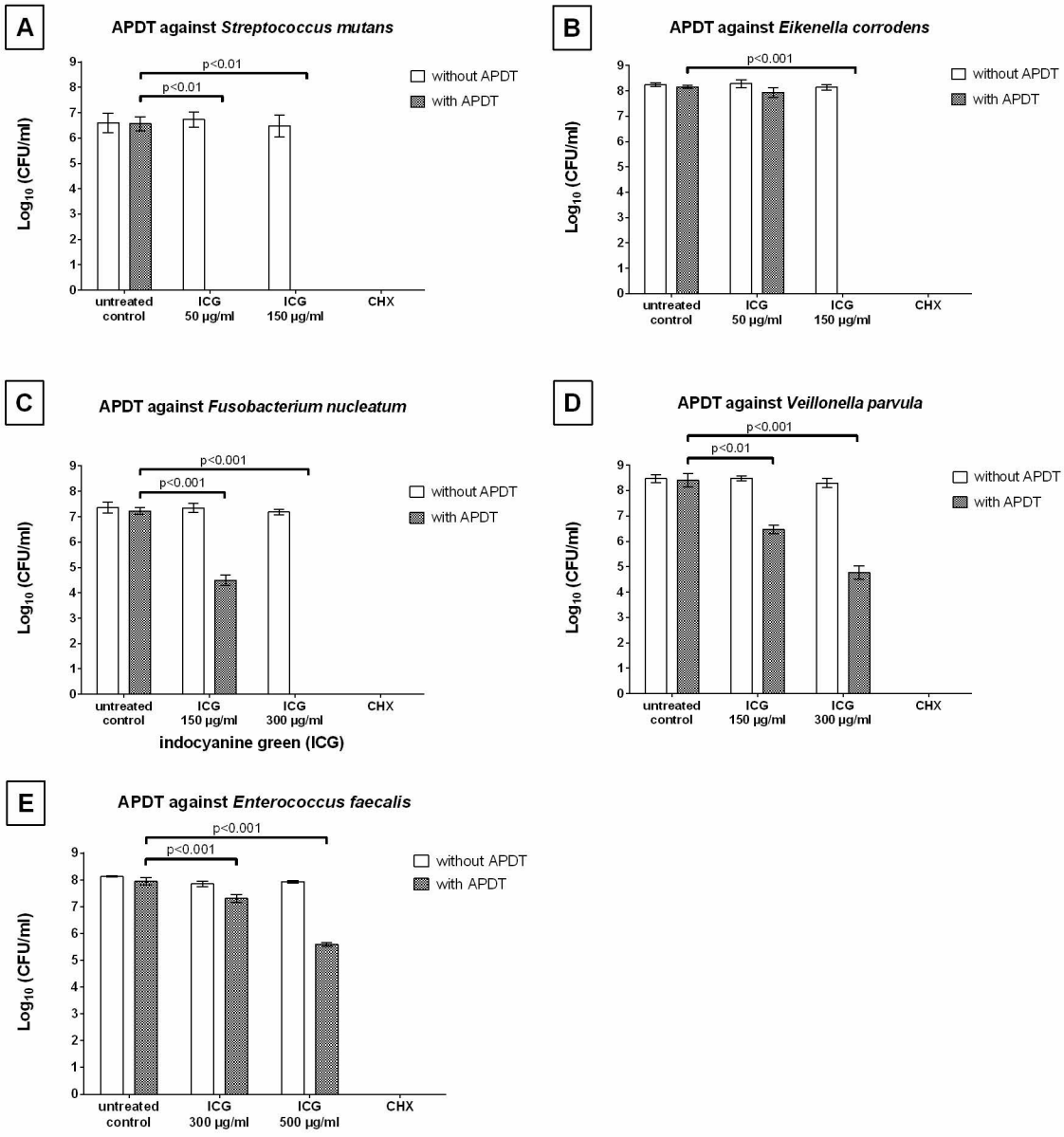
A
APDT against Streptococcus mutans
p<0.01
p<0.01
without APDT
with APDT
Log10 (CFU/ml)
untreated control
ICG 50 µg/ml
ICG 150 µg/ml
CHX
B
APDT against Eikenella corrodens
p<0.001
without APDT
with APDT
Log10 (CFU/ml)
untreated control
ICG 50 µg/ml
ICG 150 µg/ml
CHX
C
APDT against Fusobacterium nucleatum
p<0.001
p<0.001
without APDT
with APDT
Log10 (CFU/ml)
untreated control
ICG 150 µg/ml
ICG 300 µg/ml
CHX
indocyanine green (ICG)
D
APDT against Veillonella parvula
p<0.001
p<0.01
without APDT
with APDT
Log10 (CFU/ml)
untreated control
ICG 150 µg/ml
ICG 300 µg/ml
CHX
E
APDT against Enterococcus faecalis
p<0.001
p<0.001
without APDT
with APDT
Log10 (CFU/ml)
untreated control
ICG 300 µg/ml
ICG 500 µg/ml
CHX

FIG 5

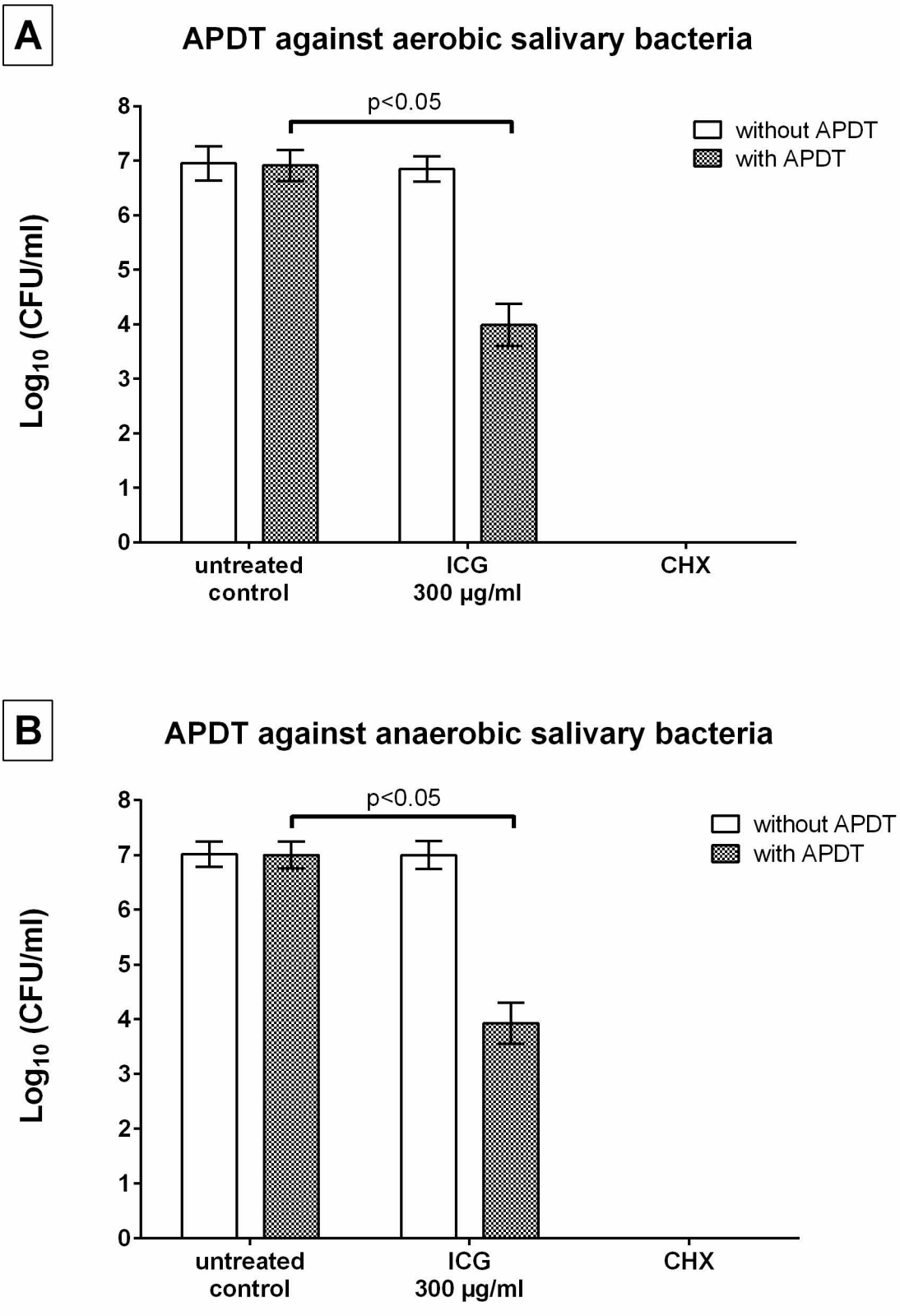
A
APDT against aerobic salivary bacteria
p<0.05
without APDT
with APDT
Log10 (CFU/ml)
0
1
2
3
4
5
6
7
8
untreated control
ICG 300 µg/ml
CHX
B
APDT against anaerobic salivary bacteria
p<0.05
without APDT
with APDT
Log10 (CFU/ml)
0
1
2
3
4
5
6
7
8
untreated control
ICG 300 µg/ml
CHX

FIG 6

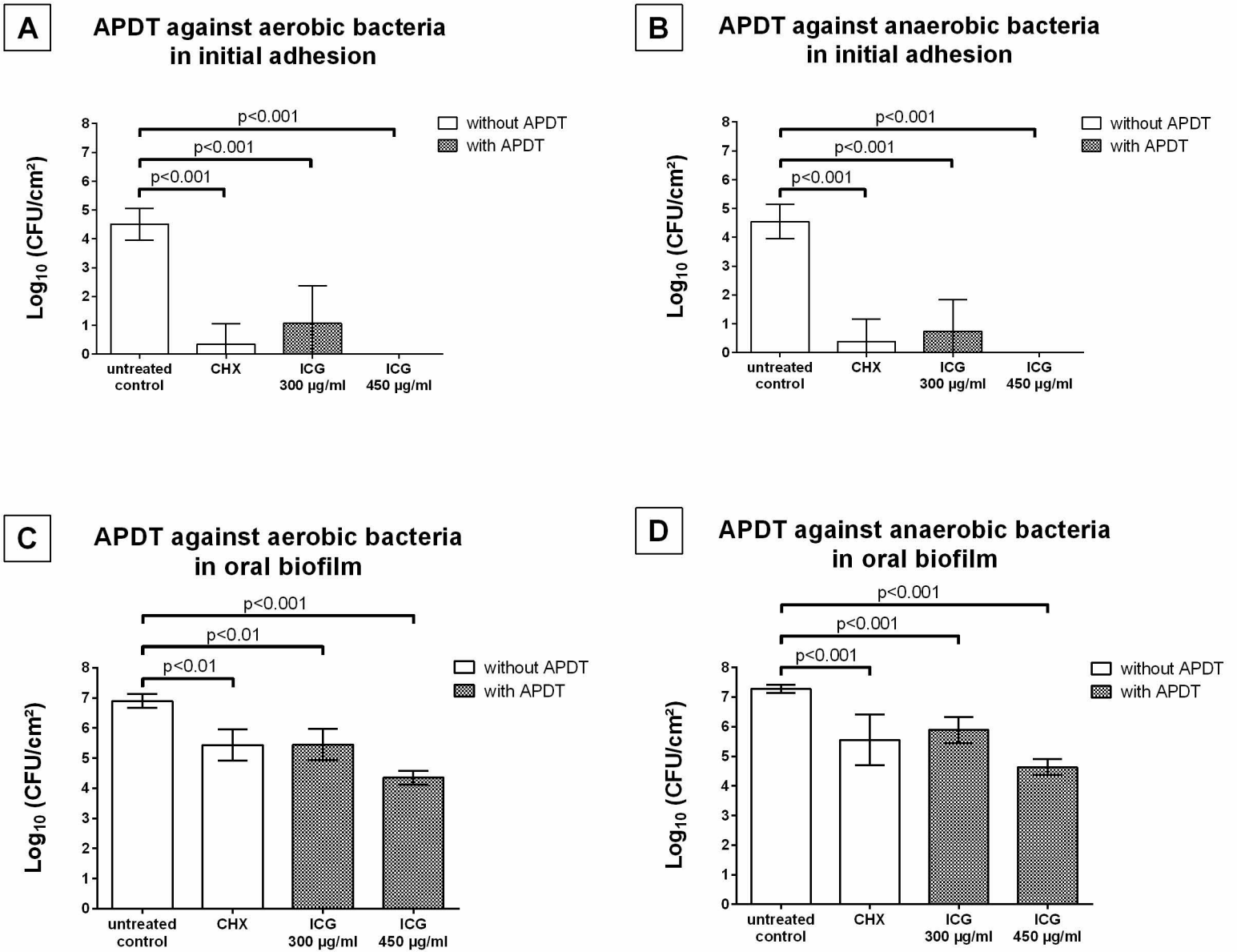
A
APDT against aerobic bacteria in initial adhesion
p<0.001
p<0.001
p<0.001
without APDT
with APDT
Log10 (CFU/cm²)
untreated control
CHX
ICG 300 µg/ml
ICG 450 µg/ml
B
APDT against anaerobic bacteria in initial adhesion
p<0.001
p<0.001
p<0.001
without APDT
with APDT
Log10 (CFU/cm²)
untreated control
CHX
ICG 300 µg/ml
ICG 450 µg/ml
C
APDT against aerobic bacteria in oral biofilm
p<0.001
p<0.01
p<0.01
without APDT
with APDT
Log10 (CFU/cm²)
untreated control
CHX
ICG 300 µg/ml
ICG 450 µg/ml
D
APDT against anaerobic bacteria in oral biofilm
p<0.001
p<0.001
p<0.001
without APDT
with APDT
Log10 (CFU/cm²)
untreated control
CHX
ICG 300 µg/ml
ICG 450 µg/ml

FIG 7

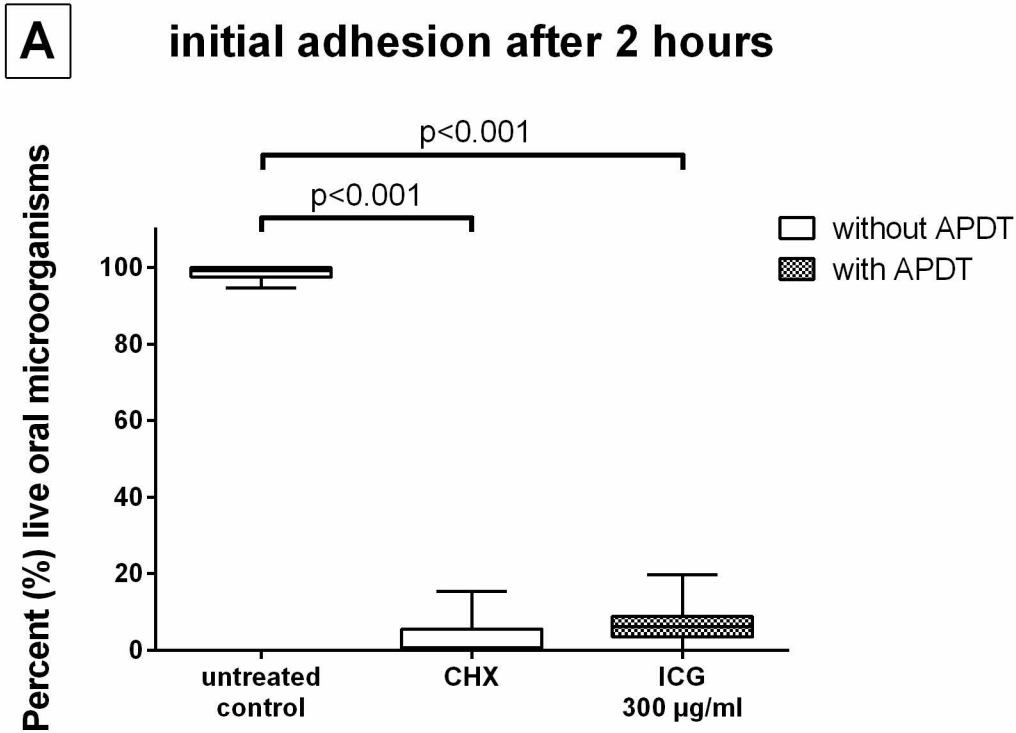
A
initial adhesion after 2 hours
p<0.001
p<0.001
without APDT
with APDT
Percent (%) live oral microorganisms
100
80
60
40
20
0
untreated control
CHX
ICG 300 µg/ml

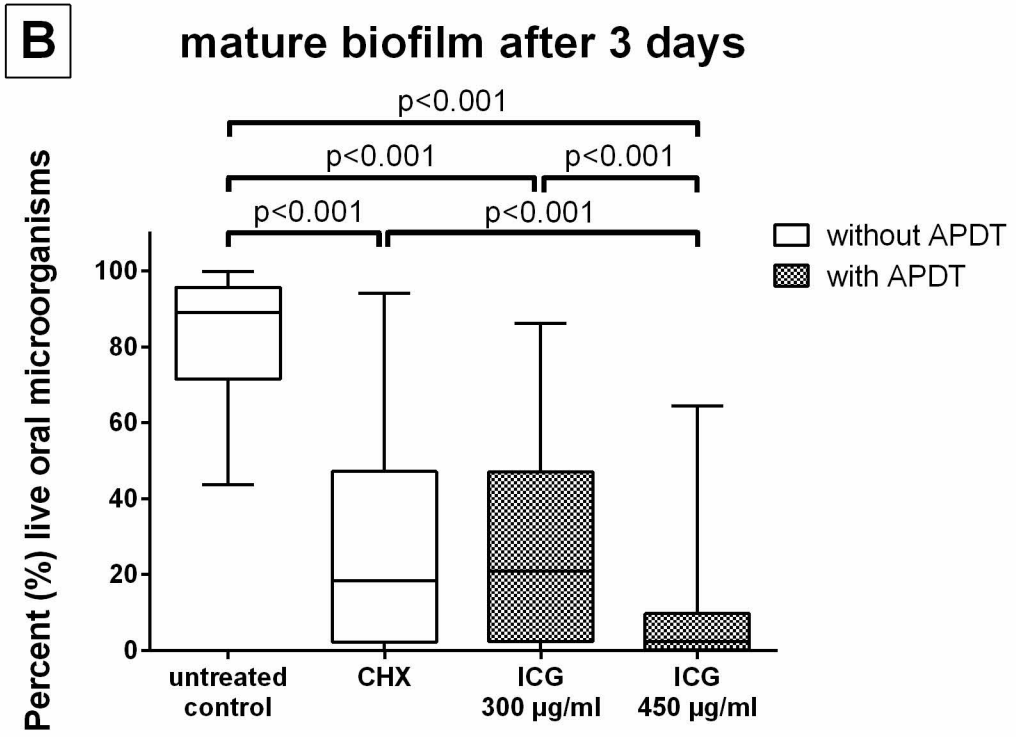
B
mature biofilm after 3 days
p<0.001
p<0.001
p<0.001
p<0.001
p<0.001
without APDT
with APDT
Percent (%) live oral microorganisms
100
80
60
40
20
0
untreated control
CHX
ICG 300 µg/ml
ICG 450 µg/ml

FIG 8

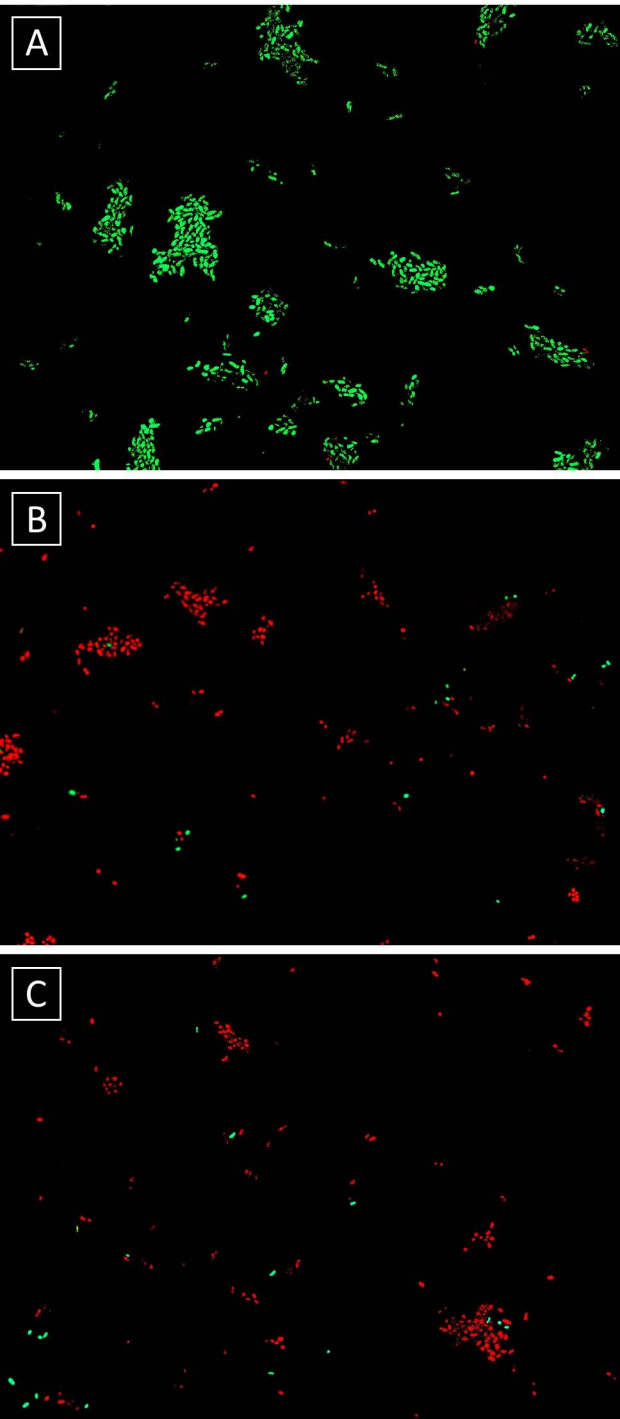

FIG 9

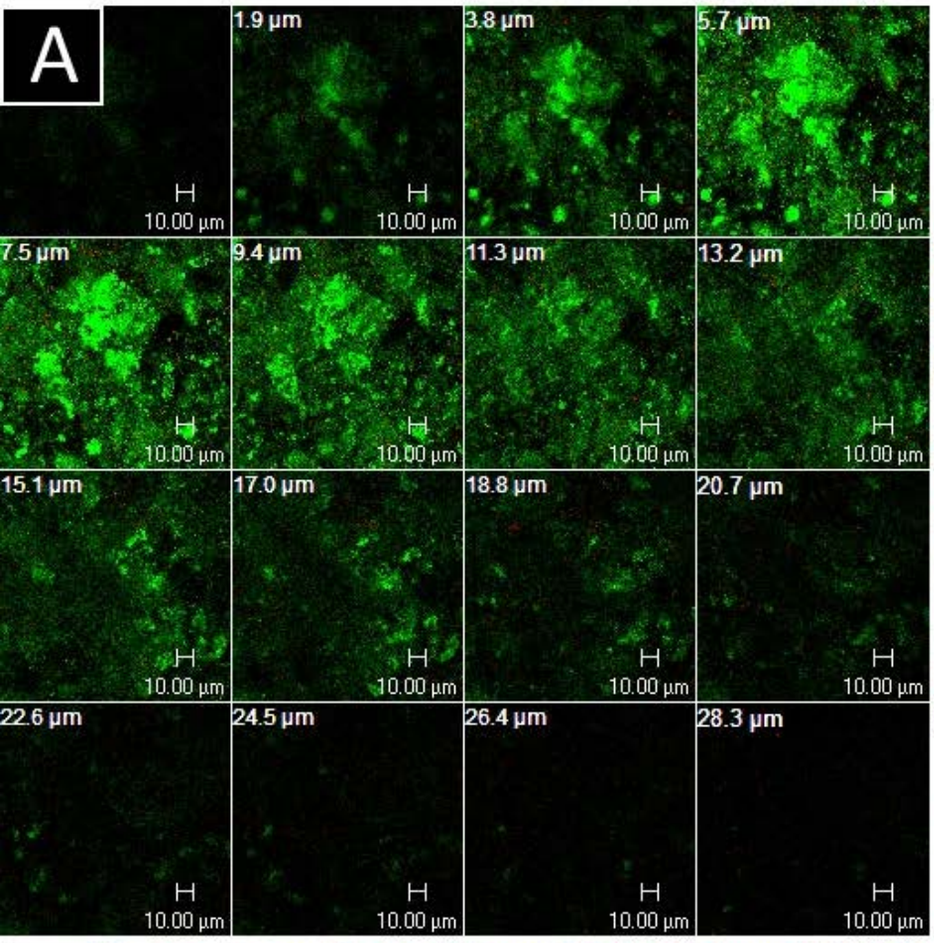
A
1.9 µm
3.8 µm
5.7 µm
7.5 µm
9.4 µm
11.3 µm
13.2 µm
15.1 µm
17.0 µm
18.8 µm
20.7 µm
22.6 µm
24.5 µm
26.4 µm
28.3 µm
10.00 µm

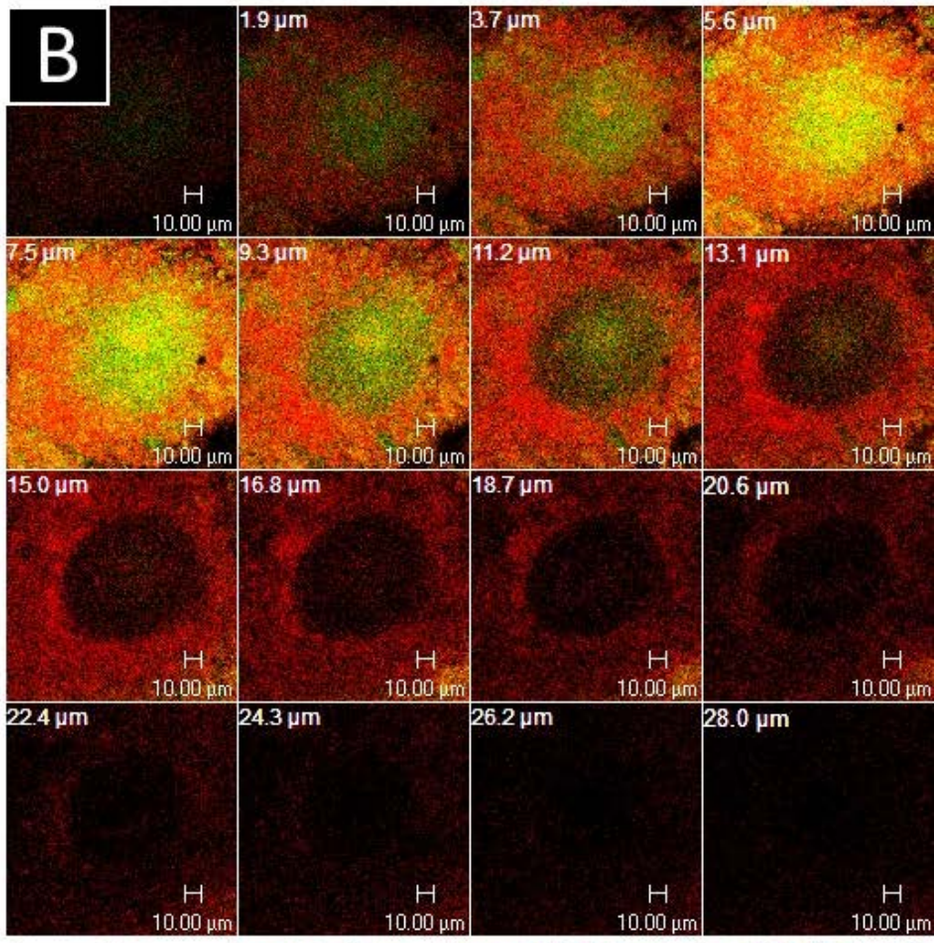
B
1.9 µm
3.7 µm
5.6 µm
7.5 µm
9.3 µm
11.2 µm
13.1 µm
15.0 µm
16.8 µm
18.7 µm
20.6 µm
22.4 µm
24.3 µm
26.2 µm
28.0 µm
10.00 µm

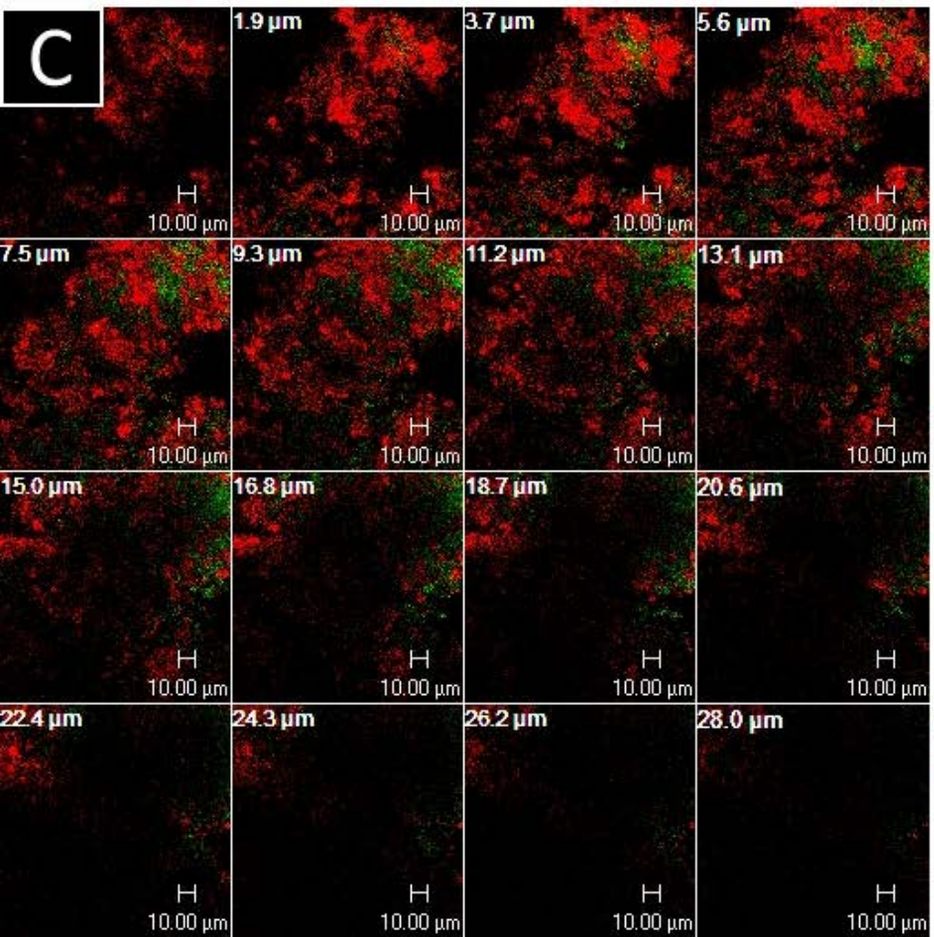
C
1.9 µm
3.7 µm
5.6 µm
7.5 µm
9.3 µm
11.2 µm
13.1 µm
15.0 µm
16.8 µm
18.7 µm
20.6 µm
22.4 µm
24.3 µm
26.2 µm
28.0 µm
10.00 µm

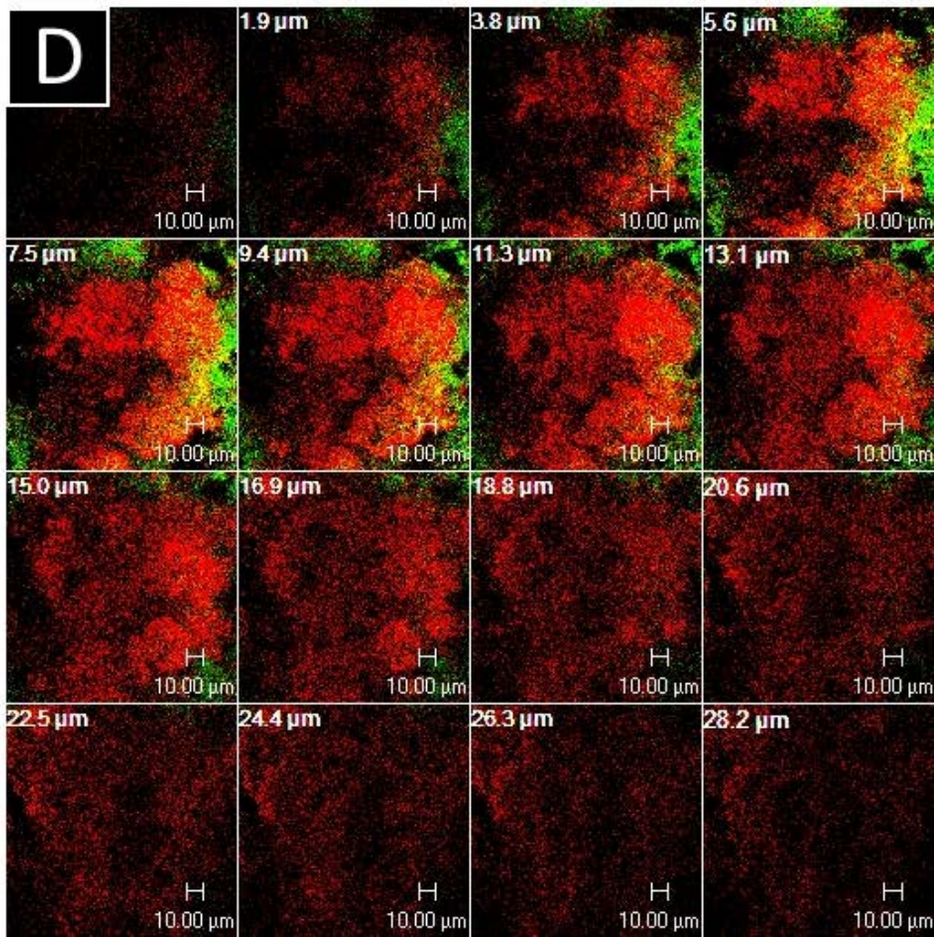
D
1.9 µm
3.8 µm
5.6 µm
7.5 µm
9.4 µm
11.3 µm
13.1 µm
15.0 µm
16.9 µm
18.8 µm
20.6 µm
22.5 µm
24.4 µm
26.3 µm
28.2 µm
10.00 µm